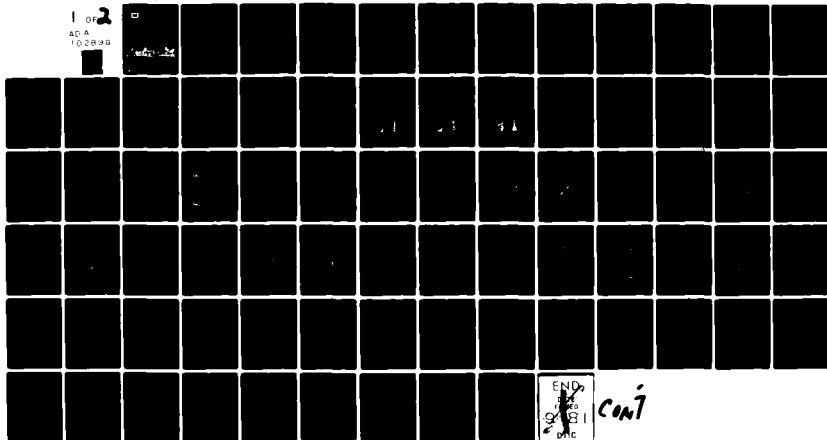


AD-A102 899 ARMY ENGINEER WATERWAYS EXPERIMENT STATION VICKSBURG--ETC F/6 8/11  
SITE EFFECTS ON POWER SPECTRAL DENSITIES AND SCALING FACTORS.(U)  
JUL 81 F K CHANG  
UNCLASSIFIED WES/MP/GL-81-2

1 of 2  
AD A  
10-28-98



cont

AD A102899



LEVEL

2



MISCELLANEOUS PAPER GL-81-2

# SITE EFFECTS ON POWER SPECTRAL DENSITIES AND SCALING FACTORS

by

Frank K. Chang

Geotechnical Laboratory  
U. S. Army Engineer Waterways Experiment Station  
P. O. Box 631, Vicksburg, Miss. 39180

July 1981

Final Report

Approved For Public Release; Distribution Unlimited

DTIC  
AUG 18 1981  
H



Prepared for Office, Chief of Engineers, U. S. Army  
Washington, D. C. 20314

Under Project 4A161102AT22, Work Unit 00296

DTIC FILE COPY

81 8 17 112

Destroy this report when no longer needed. Do not return  
it to the originator.

The findings in this report are not to be construed as an official  
Department of the Army position unless so designated,  
by other authorized documents.

The contents of this report are not to be used for  
advertising, publication, or promotional purposes.  
Citation of trade names does not constitute an  
official endorsement or approval of the use of  
such commercial products.

Unclassified

SECURITY CLASSIFICATION OF THIS PAGE (When Data Entered)

REPORT DOCUMENTATION PAGE		READ INSTRUCTIONS BEFORE COMPLETING FORM
1. REPORT NUMBER Miscellaneous Paper GL-81-2	2. GOVT ACCESSION NO. AD-A102 899	3. RECIPIENT'S CATALOG NUMBER
4. TITLE (and Subtitle) SITE EFFECTS ON POWER SPECTRAL DENSITIES AND SCALING FACTORS.	5. TYPE OF REPORT & PERIOD COVERED Final report.	6. PERFORMING ORG. REPORT NUMBER
7. AUTHOR(s) Frank K. Chang	8. CONTRACT OR GRANT NUMBER(s)	9. PROGRAM ELEMENT, PROJECT, TASK AREA & WORK UNIT NUMBERS Project 4A161102AT22 Work Unit 00296
10. PERFORMING ORGANIZATION NAME AND ADDRESS U. S. Army Engineer Waterways Experiment Station Geotechnical Laboratory P. O. Box 631, Vicksburg, Miss. 39180	11. CONTROLLING OFFICE NAME AND ADDRESS Office, Chief of Engineers, U. S. Army Washington, D. C. 20314	12. REPORT DATE Jul 81
13. MONITORING AGENCY NAME & ADDRESS (if different from Controlling Office)	14. NUMBER OF PAGES 72	15. SECURITY CLASS. (of this report) Unclassified
16. DISTRIBUTION STATEMENT (of this Report) Approved for public release; distribution unlimited.		17. SECURITY CLASS. (of this report) Unclassified
18. DISTRIBUTION STATEMENT (of the abstract entered in Block 20, if different from Report)		
19. SUPPLEMENTARY NOTES Available from National Technical Information Service, 5285 Port Royal Road, Springfield, Va. 22151.		
20. KEY WORDS (Continue on reverse side if necessary and identify by block number) Accelerograms                      Spectrum analysis Earthquake engineering              Statistical analysis Power spectra		
21. ABSTRACT (Continue on reverse side if necessary and identify by block number) This study presents the results of a statistical analysis of the spectral shapes of power spectral density (PSD) functions, $G(u)$ , in the 0.006- to 10-Hz range for 421 horizontal ground accelerograms (all records processed to the same duration of 163.83 sec, i.e., $1/163.82 = 0.006$ Hz) from 89 earthquakes, mostly in the western United States and Japan. The analysis shows clear differences in spectral shapes for different soil and geological conditions. Within the high- frequency range of 2.5 to 10 Hz, the spectrum for the rock sites contains the (Continued)		

DD FORM 1 JAN 73 1473

EDITION OF 1 NOV 65 IS OBSOLETE

Unclassified

SECURITY CLASSIFICATION OF THIS PAGE (When Data Entered)

41172

Unclassified

SECURITY CLASSIFICATION OF THIS PAGE(When Data Entered)

20. ABSTRACT (Continued).

highest energy or intensity; the spectrum of the stiff soil sites is slightly less than for the rock sites; and the spectra of the soft clay and sand sites and the deep cohesionless soil sites are almost the same and are lower than those for stiff soils. However, in the low-frequency range of 0.006 to 2.5 Hz, the reverse exists: the soft sites indicate the highest energy, the deep cohesionless soil sites are next, the stiff soil sites are third, and finally, the rock sites.

A qualitative comparison was made of the spectral shapes of the PSD calculated in this study with the acceleration response spectra (ARS) of Kiremidjian and Shah (1978), Seed and Idriss (1971), and Seed, Ugas, and Lysmer (1976). There is general agreement in the shapes of both types of spectra, except the relative amplitudes for the rock sites for the ARS were less than those of the PSD in the high-frequency range. The difference in relative amplitudes for the rock PSD and ARS is due principally to the lesser number of records used in the data analysis for the latter. The number of records for the rock sites was 28 for the ARS and 56 for the PSD. Another difference is that the spectral shapes of PSD functions show more peaks than do the ARS, i.e., ARS are smoother. Above all, both differences could be affected by the frequency increment and the smoothing technique.

The average and average plus one standard deviation power density spectra functions for different site conditions have been normalized to a unit area. Based on these normalized PSD standard spectra and amplification scaling curves, which are derived from the average power  $\lambda^2$ , the area under  $G(\omega)$ , or its square root, the rms (root-mean-square) value ( $\lambda$ ) developed in this study, a design earthquake PSD spectrum for any earthquake magnitude and distance can be generated. These scaling curves, i.e., the correlation curves of peak ground acceleration or peak velocity versus rms value, and rms value versus Modified Mercalli Intensity, can also serve as earthquake engineering intensity scales in a quantitative manner.

Unclassified

SECURITY CLASSIFICATION OF THIS PAGE(When Data Entered)

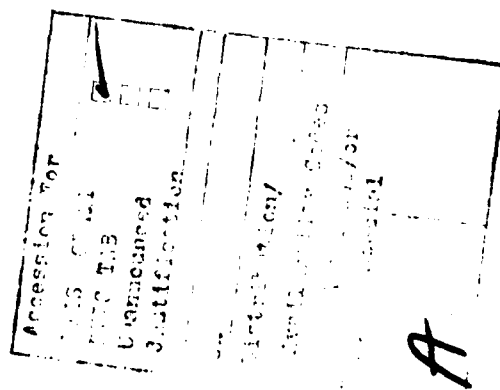
## PREFACE

This study was conducted as a part of the work at the U. S. Army Engineer Waterways Experiment Station (WES) in the Military Works Program, Project 4A161102AT22, Work Unit 00296, which was monitored for the Office, Chief of Engineers, U. S. Army, by Mr. A. F. Muller.

This report was prepared by Mr. Frank K. Chang of the Earthquake Engineering and Geophysics Division (EE&GD), Geotechnical Laboratory (GL), under the general direction of Dr. A. G. Franklin, Principal Investigator; Dr. P. F. Hadala, Assistant Chief, GL; and Mr. C. L. McAnear, Acting Chief, GL.

The author would like to make special acknowledgements to Mr. Mike Landau, Assistant Analyst, Potomac Research, Consultants to the WES ADP Center, for his help in the data processing; Mr. Tatsuo Uwabe, visiting Research Engineer from the Port and Harbour Research Institute (PHRI), Japan, who provided the digitized Japanese strong-motion accelerograms of 1963 to 1975 recorded by the PHRI and the geological site conditions associated with each record; Professor M. Shinozuka, Columbia University, who provided the computer program used to calculate the one-sided PSD functions; Professor O. W. Nuttli, Saint Louis University, who made some comments for the first draft of this report; Professor E. H. Vanmarcke and Dr. Shih-Sheng (Paul) Lai, Massachusetts Institute of Technology; Professor H. C. Shah, Stanford University; Dr. S. C. Liu, National Science Foundation; and Drs. P. F. Hadala, W. F. Marcuson, and A. G. Franklin, WES, who made the critical reviews for this final report.

Commanders and Directors of WES during the period of this study were COL John L. Cannon, CE, and COL Nelson P. Conover, CE. Technical Director was Mr. F. R. Brown.



# CONTENTS

	<u>Page</u>
PREFACE . . . . .	1
PART I: INTRODUCTION . . . . .	3
Background . . . . .	3
Purpose and Scope . . . . .	5
PART II: POWER SPECTRAL DENSITY . . . . .	6
Fourier Transform . . . . .	6
Total Intensity, Average Power, and PSD . . . . .	7
Strong-Motion Duration and Normalized PSD . . . . .	8
Summary of Mathematical Relations . . . . .	10
PART III: DATA SELECTION AND DATA PROCESSING . . . . .	12
Data Selection . . . . .	12
Definition of Average Power and Average Acceleration . . . . .	12
Spectral Smoothing . . . . .	12
Statistical Errors . . . . .	13
Record Length, Increment Frequency, and NPSD Function . . . . .	14
Spectral Frequency Range . . . . .	18
Computer Procedures for Generating PSD . . . . .	18
PART IV: DATA PRESENTATION . . . . .	20
PART V: DATA ANALYSES . . . . .	23
Analysis of Site-Dependent PSD Spectral Shape . . . . .	23
Statistical Characteristics of the Earthquake	
Ground Motions . . . . .	27
Maximum Ground Acceleration and Average Acceleration . . . . .	28
Peak Factor . . . . .	28
Comparison of Average Acceleration and Peak Ground	
Acceleration Versus Distance . . . . .	37
Potential Uses of Site-Dependent Standard NPSD	
Spectral Curves . . . . .	40
Peak Velocity Versus Average Acceleration . . . . .	43
Correlation of Average Acceleration and Modified	
Mercalli Intensity . . . . .	45
Correlation of $I_0$ and MMI . . . . .	45
PART VI: SUMMARY, CONCLUSIONS, AND RECOMMENDATIONS . . . . .	51
Summary . . . . .	51
Conclusions . . . . .	53
Recommendations . . . . .	54
REFERENCES . . . . .	55
TABLES 1-8	

SITE EFFECTS ON POWER SPECTRAL DENSITIES  
AND SCALING FACTORS

PART I: INTRODUCTION

Background

1. Three ways of expressing the characteristics of earthquake ground motion in the frequency domain are to compute the peak response spectrum, Fourier spectra, and power spectral density (PSD). The response spectrum represents the peak response of a linear 1-degree-of-freedom system to the ground motion and provides a convenient method of obtaining a preliminary analysis of certain structural dynamics problems. The PSD is related to the Fourier amplitude spectrum of the ground motion. In fact, the three are closely related.

2. Both response spectrum and PSD functions have been widely used to describe earthquake ground motions in the frequency domain. Pereira, Oliveira, and Duarte (1977), Vanmarcke and Cornell (1972), and Vanmarcke and Gasparini (1977) have shown that the PSD function, the acceleration-time plots, and the response spectra are all interrelated. Thus, if a design level response spectrum is specified, then an equivalent PSD function and a set of corresponding acceleration-time curves that are consistent with the response spectrum can be generated. However, neither the PSD nor the response spectrum can uniquely determine the acceleration-time curve, because both are incomplete representations of the ground motion, lacking phase information.

3. Seed and Idriss (1971), Tezcan (1971), and many others have confirmed that damage to buildings during past earthquakes has been closely associated with the vibrational characteristics of the underlying soils. Duke and Hradilek (1977) and Berrill (1977) utilized Fourier spectra to study the effects of local site conditions on ground motions recorded in the 9 February 1971 San Fernando earthquake and its aftershocks. However, no positive correlations were found. Hudson (1972)



and Hudson and Udwadia (1974) made a comparison of measured strong ground motions in the form of plots of Fourier spectra at selected sites and found that various governing factors could be individually studied; and in this way, it was shown that local variations are largely governed by (a) source mechanisms, (b) propagation path, and (c) local geology.

4. Seed, Ugas, and Lysmer (1976) presented the results of a statistical analysis of the response spectral shapes of 104 ground-motion accelerograms obtained from 23 earthquakes, mostly in the western United States. The analysis shows clear differences in spectral shapes for different soil and geological conditions. Chang and Krinitzsky (1977) studied the duration and spectral content of strong-motion records from the western United States according to site conditions and found that the predominant frequencies are in the range of 0.1 to 6.67 Hz and the spectral shape depends on the source spectrum function (magnitude), distance, and geological conditions.

5. An extensive study was made at the strong-motion station sites in Ferndale and El Centro, California, by Shannon and Wilson, Inc./ Agbabian Associates (1976). Both sites are located in a highly seismic region and have many ground-motion records. The subsurface conditions at these sites were defined by geotechnical investigations that included boring and sampling of the subsurface soil materials followed by field and laboratory tests to define the index properties and the dynamic properties of the soil needed for one-dimensional wave propagation analyses by numerical methods. The site-response analysis (SHAKE code), site-matched records, Seed-Ugas-Lysmer site dependent spectrum, Nuclear Commission Regulatory Guide 1.60 spectrum, and spectra from the measured records that correspond to the "design" earthquake event for the site were studied. No single method yielded the best vibratory motion criteria for both sites. The methods described above have limitations that either are related to the simplified models used for site-response wave propagation analyses or are a direct result of the limitations in the current library of strong-motion records.

6. Considering the earthquake ground motion to be random in

nature, Arnold (1975) and Arnold and Vanmarcke (1977) studied the influence of site azimuth relative to source fault orientation and local soil conditions on earthquake ground-motion spectra for the San Fernando, California, earthquake of 9 February 1971 using PSD functions. The result showed that local soil conditions and site azimuth, as well as epicentral distance, can have a significant effect on both the intensity and the frequency content of ground motions. This study demonstrated the potential value of PSD functions as a tool for comparing and studying variations in ground-motion characteristics and also showed the great utility of PSD functions as input to random vibration analyses of structural response.

#### Purpose and Scope

7. The main purpose of this study is to analyze the site dependence of PSD shapes in the frequency range of 0 to 10 Hz and to consider the application of PSD shapes in seismic design. Knowledge of the influence of site conditions on the characteristics of earthquake ground motions and their spectral shapes is necessary for earthquake-resistant design and analysis of structures such as earth, rockfill, or concrete dams, large buildings, nuclear power plants, and other military or civil facilities.

8. Factors affecting the ground motion at a particular site include the source mechanism (nature of fault movement and magnitude of energy release), propagation path characteristics, the direction of the site relative to the fault rupture, and local geological and soil conditions. This study, however, deals only with the influence of local geological and soil conditions on ground motion.

## PART II: POWER SPECTRAL DENSITY

9. In the application of the random vibration theory of linear systems for evaluation of the effects of variations in ground-motion characteristics on structural response to earthquake excitation, the ground motion may be described in the form of a PSD function. The PSD function  $G(\omega)$  is defined as a measure of the ground-motion power or energy per unit time as a function of frequency  $\omega$  (Figure 1). Usually, estimates of the PSD are obtained from the squared amplitudes of the Fourier transform, or the squared Fourier amplitude spectrum. In Figure 1,  $A_i$  is the amplitude of sinusoidal waves.

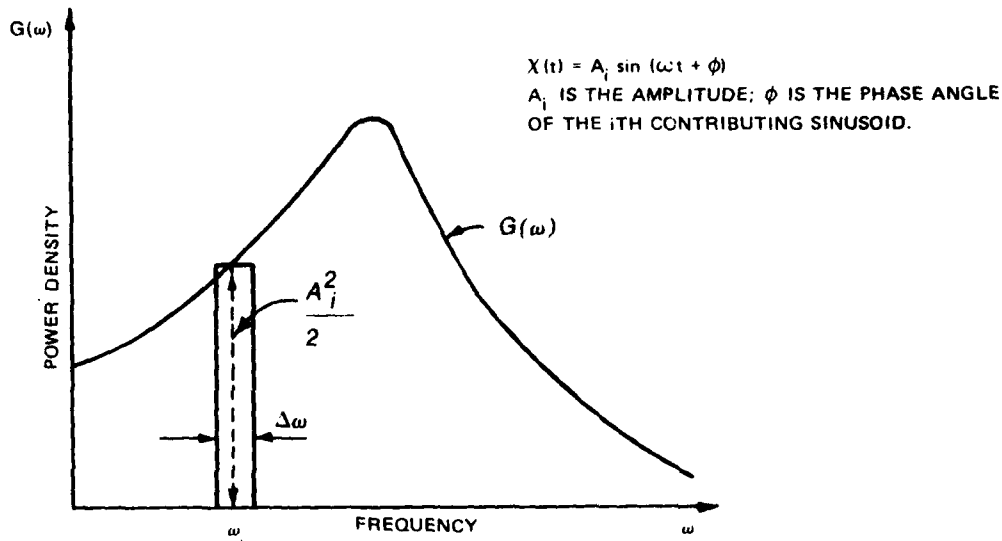


Figure 1. The PSD function  $G(\omega)$

### Fourier Transform

10. Generally, the given earthquake ground-motion function, such as an acceleration versus time plot, can be represented in the time domain as  $a(t)$  and in the frequency domain as  $F(\omega)$  :

$$F(\omega) = \int_0^{t_0} a(t) e^{-i\omega t} dt, \quad i = \sqrt{-1} \quad (1)$$

and

$$a(t) = \frac{1}{\pi} \int_{\omega_1}^{\omega_0} F(\omega) e^{i\omega t} d\omega, \quad i = \sqrt{-1} \quad (2)$$

Equations 1 and 2 are called the Fourier transform pair; i.e.,  $F(\omega)$  is the Fourier integral or Fourier transform of  $a(t)$ , and  $a(t)$  is the inverse Fourier transform of  $F(\omega)$ . The symbols  $t$  and  $t_0$  denote the instant in time and total duration, and  $\omega$ ,  $\omega_1$ , and  $\omega_0$  represent the frequency, lower frequency bound  $\omega_1 = 2\pi/t_0$ , and maximum frequency (in radians per second), respectively. For practical purposes,  $\omega_1$  can usually be taken as zero.

#### Total Intensity, Average Power, and PSD

11. By Parseval's theorem, the relation between the energy of the motion as expressed in the time domain and in the frequency domain can be represented in the following equations. For a nonperiodic function, the total energy or intensity  $I_0$  delivered by the source is given by

$$I_0 = \int_0^{t_0} |a(t)|^2 dt = \frac{1}{\pi} \int_0^{\omega_0} |F(\omega)|^2 d\omega \quad (3)$$

The mean-square average value is expressed

$$\frac{1}{t_0} \int_0^{t_0} |a(t)|^2 dt = \frac{1}{\pi} \frac{1}{t_0} \int_0^{\omega_0} |F(\omega)|^2 d\omega = \int_0^{\omega_0} G(\omega) d\omega \quad (4)$$

in which  $G(\omega)$  is the energy per unit time (power), or the power spectral density of the function  $a(t)$ . The integrand on the right side of Equation 4 can be written as

$$G(\omega) = \frac{1}{\pi} \frac{1}{S_0} |F(\omega)|^2 \quad (5)$$

if  $S_0$  (duration of strong motion) is substituted for  $t_0$ , and

$$\frac{1}{\pi} \int_0^{\omega_0} |F(\omega)|^2 d\omega = S_0 \int_0^{\omega_0} G(\omega) d\omega$$

The quantity  $|F(\omega)|^2$  is called the energy spectrum or energy spectral density function of  $a(t)$  (Hsu 1967). The left side of Equation 4 gives the statistical average power  $\lambda_0^2$  of the function  $a(t)$  over the total duration of the motion  $t_0$ . From Equation 4, also note that  $\lambda_0^2$  is equal to the area under the curve of  $G(\omega)$  in Figure 1. Therefore, the average power can be written as

$$\lambda_0^2 = \int_0^{\omega_0} G(\omega) d\omega \quad (6)$$

#### Strong-Motion Duration and Normalized PSD

12. From the relation of Equations 3, 4, 5, and 6, the total intensity  $I_0$  can be expressed as

$$I_0 = S_0 \lambda_0^2 \quad (7a)$$

or

$$S_0 = \frac{I_0}{\lambda_0^2} \quad (7b)$$

A peak factor  $r$  may be defined as

$$r = \frac{a_{\max}}{\lambda_o} \quad (8a)$$

or

$$\lambda_o = \frac{a_{\max}}{r} \quad (8b)$$

Therefore, by substitution

$$S_o = r^2 \frac{I_o}{a_{\max}^2} \quad (9)$$

where  $r$ , which is a dimensionless parameter, can be determined empirically. This equation gives the strong-motion duration  $S_o$ , defined by Vanmarcke and Lai (1977), which is necessarily smaller than the total duration  $t_o$ . The PSD values in this report are computed in terms of  $t_o$ , which yields smaller PSD values.

13. A more effective way for dealing with the frequency content of ground motion is through the normalized spectral density function  $G^*(\omega)$ :

$$G^*(\omega) = \frac{1}{\lambda_o^2} G(\omega) \quad (10)$$

If  $G_i^*(\omega)$  is an individual normalized PSD function, the statistical mean PSD curve will be

$$\bar{G}^*(\omega) = \frac{1}{n} \sum_{i=1}^n G_i^*(\omega), \quad i = 1, 2, \dots, n \quad (11)$$

In practice, curves of  $\bar{G}^*(\omega)$  computed from suites of actual earthquake records show large and irregular fluctuations. To isolate the systematic component from the random variations, frequency smoothing with a "Hanning" window (Blackman and Tukey 1958) should be used. A detailed

procedure for the frequency smoothing will be presented in Part III.

### Summary of Mathematical Relations

14. The above mathematical and logical presentations can be outlined as follows:

#### Time domain

#### Frequency domain

Fourier transform pair:

$$a(t) = \frac{1}{\pi} \int_0^{\omega_0} F(\omega) e^{i\omega t} d\omega ;$$

$$F(\omega) = \int_0^{t_0} a(t) e^{-i\omega t} dt \quad (12a, b)$$

$\omega_0$  = maximum frequency

$t_0$  = total duration

Total intensity:

$$I_0 = \int_0^{t_0} |a(t)|^2 dt ;$$

$$I_0 = \frac{1}{\pi} \int_0^{\omega_0} |F(\omega)|^2 d\omega \quad (13a, b)$$

Average power:

$$\lambda_0^2 = \frac{1}{t_0} \int_0^{t_0} |a(t)|^2 dt ;$$

$$\lambda_0^2 = \int_0^{\omega_0} G(\omega) d\omega \quad (14a, b)$$

Power spectral density:

---

$$G(\omega) = \frac{1}{\pi} \frac{1}{S_0} |F(\omega)|^2, \quad S_0 \rightarrow t_0^*$$

---

\* Either total duration  $t_0$  or strong-motion duration  $S_0$  (Vanmarcke and Lai 1977) may be used. In this study,  $t_0$  is generally used.

Average acceleration:

$$\lambda_o = \left[ \frac{1}{t_o} \int_0^{t_o} |a(t)|^2 dt \right]^{1/2} \quad \lambda_o = \left[ \int_0^{\omega_o} G(\omega) d\omega \right]^{1/2} \quad (15a, b)$$

Strong-motion duration:

$$S_o = \frac{I_o}{\lambda_o^2} \quad S_o = \frac{I_o}{\lambda_o^2} \quad (16)$$

15. This study includes investigation of (a) the site dependence of the PSD's or the power spectral shapes in the frequency range of 0 to 10 Hz for four general types of site conditions, which are classified as rock, stiff soil, deep cohesionless soil, and soft soil; (b) the statistical characteristics of the ground motions; (c) the relations between the power spectrum, average acceleration, average power (scaling factor), duration, and total intensity (Arias); and (d) the development of average acceleration as an alternative earthquake engineering intensity scale. The average acceleration not only describes the intensity of ground motion for input to structural design but also serves as the scaling factor ( $\lambda_o^2$ ) of the normalized standard PSD spectra. In this report, duration will be considered in a general sense; the strong-motion duration will not be defined.



## PART III: DATA SELECTION AND DATA PROCESSING

### Data Selection

16. A total of 421 horizontal ground accelerograms from 89 earthquakes, mostly in the western United States and Japan (with a few records from Russia, Rumania, and India), were selected for this analysis. Based on the site classifications of Seed and Idriss (1971) and Seed, Ugas, and Lysmer (1976), these records have been divided into four groups: (a) 56 records for rock sites, (b) 131 records for stiff soil sites (depth <150 ft), (c) 120 records for deep cohesionless soil sites (depth >250 ft), and (d) 114 records for soft to medium clays with associated strata of sands or gravels. One hundred seventy-three of the 421 records were obtained from California Institute of Technology (CIT) Volume II-Corrected Accelerograms (1971-75), and 220 uncorrected records were provided by the Port and Harbour Research Institute (PHRI), Japan. The digitized Gazli (USSR) and Bucharest (Rumania) records were provided by Dr. A. G. Brady, U. S. Geological Survey. All 421 corrected and uncorrected records were adjusted to zero mean before processing the PSD.

### Definition of Average Power and Average Acceleration

17. The main approach used in this study was to determine the normalized mean and the mean plus one standard deviation PSD shape (NPSD) for each group, and the average acceleration  $\lambda_o$  using Equation 15b, for each raw record. Figure 1 shows  $G(\omega)$ , whose value at  $\omega_i$  is equal to  $A_i^2/2\Delta\omega$ , so that  $\lambda_o^2$  is actually the power or energy density in an accelerogram for a finite frequency band ( $0 \leq f \leq 10$  Hz in this study), and  $A_i$  is the amplitude of the  $i$ th wave component in centimetres per second squared. The total or average power will become equal to the area under the continuous curve  $G(\omega)$ .

### Spectra. Smoothing

18. The statistical (mean and mean plus one standard deviation)

NPSD function shapes for each group appear very irregular. Therefore, a spectral or frequency smoothing technique has to be employed to eliminate random, or nonsystematic, fluctuations of the NPSD curve. A final smooth estimate of the NPSD may now be formed by further frequency smoothing with a procedure called the "Hanning window" by Blackman and Tukey (1958) and Bendat and Piersol (1971). Let  $\tilde{G}_K$  and  $\hat{G}_K$  denote a raw and smooth estimate at harmonic  $K$ , where  $K = 0, 1, 2, \dots, m$ ; then

$$\begin{aligned}\hat{G}_0 &= 0.5\tilde{G}_0 + 0.5\tilde{G}_1 \\ \hat{G}_K &= 0.25\tilde{G}_{K-1} + 0.5\tilde{G}_K + 0.25\tilde{G}_{K+1} \quad K = 1, 2, \dots, m+1 \\ \hat{G}_m &= 0.5\tilde{G}_{m-1} + 0.5\tilde{G}_m\end{aligned} \quad (17)$$

#### Statistical Errors

19. The descriptive properties of a random variable cannot be precisely determined from sample data. Only estimates of the parameters of interest can be obtained from a finite sample of observations. The accuracy of parameter estimates based upon sample values can be described by a mean square error defined as

$$E[(\hat{\phi} - \phi)^2] = E\left\{[\hat{\phi} - E(\hat{\phi})]^2\right\} + E\left\{[E(\hat{\phi}) - \phi]^2\right\} \quad (18)$$

where  $\hat{\phi}$  is an estimator for  $\phi$ . The first term on the right side of Equation 18 is the variance  $\text{Var}(\hat{\phi})$ , which describes the random portion of the error; the second term is the square of a bias  $b^2(\hat{\phi})$ , which describes the systematic portion of error. Therefore, the mean square error is the sum of two terms:

$$E[(\hat{\phi} - \phi)^2] = \text{Var}(\hat{\phi}) + b^2(\hat{\phi}) \quad (19)$$

and the rms error is

$$\sqrt{E[(\hat{\phi} - \phi)^2]} = \sqrt{\sigma^2(\hat{\phi}) + b^2(\hat{\phi})} \quad (20)$$

where  $\text{Var}(\hat{\phi}) = \sigma^2(\hat{\phi})$  and  $\sigma(\hat{\phi})$  equals the standard error or random error. Bendat and Piersol (1971) give the simple relationship between the random error  $E_r$  and the smoothing times  $N_d$  as  $E_r = 1/\sqrt{N_d}$ . Thus, for increasing numbers of smoothing times, the corresponding values of  $E_r$  are as follows:

$N_d$	$E_r$
25	0.20
100	0.10
500	0.045
10,000	0.01

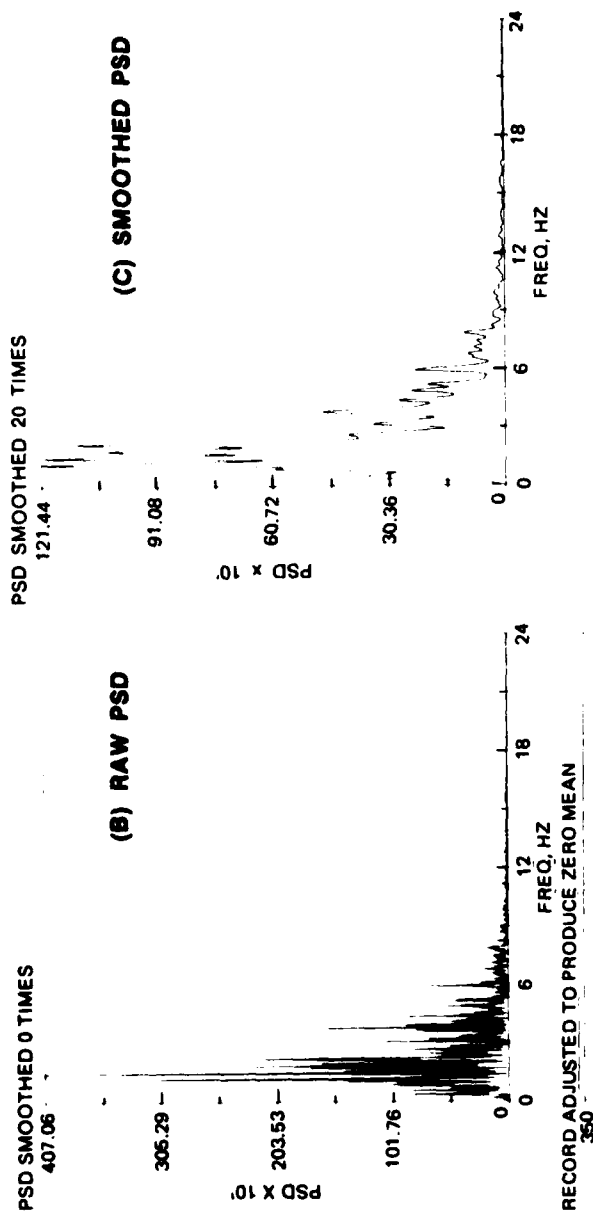
The four normalized mean and mean plus one standard deviation PSD curves in this study have been smoothed 500 times, so the random error  $E_r$  should be less than 5 percent. Figure 2 shows the effect of the smoothing process on a typical PSD.

#### Record Length, Increment Frequency, and NPSD Function

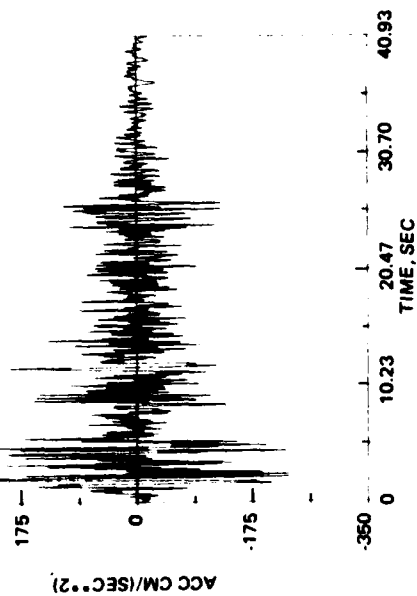
20. The record length and spectral content (spectral amplitude and frequency range) are two basic elements for controlling the spectral intensity. The incremental frequency  $\Delta f$ , used in the PSD computer program, depends on the total record length. Since it is necessary to use the same value for  $\Delta f$  throughout, all accelerograms have been processed to give them a duration of 163.82 sec or 8192 ( $2^{13}$ ) digital points with an equal time interval  $\Delta t$  of 0.02 sec, which gives  $\Delta f = 0.006104$  Hz. Outside the time of the actual record, the amplitudes at extended times were set to zero. In this study, the PSD function  $G(f)$  has been defined to include only the frequency range of 0 to 10 Hz so that

$$\lambda^2 = \int_0^{10 \text{ Hz}} G(f) df \quad (21)$$

Since  $\Delta f$  is 0.006104 Hz, there are 1640 points in the raw PSD function for each accelerogram. The NPSD function is defined as the PSD amplitude



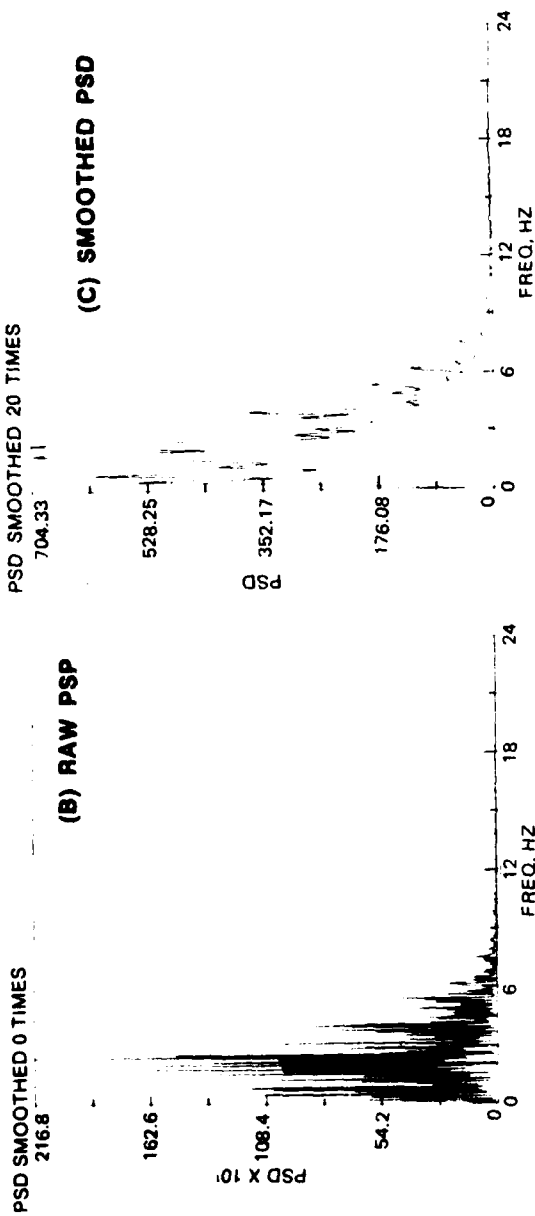
(A) ACCELEROGRAM (N-S)



IMPERIAL VALLEY EARTHQUAKE  
MAY 18, 1940 - 2037 PST  
STATION NO. 117 COMP S 00 E

a.

Figure 2. Accelerograms, and raw and smoother PSD spectra of N-S, E-W, and vertical components of El Centro earthquake, 18 May 1980 (Sheet 1 of 3)



IMPERIAL VALLEY EARTHQUAKE  
MAY 18, 1940 - 2037 PST  
STATION NO. 117 COMP S 90 W

(A) ACCELEROGRAM (E-W)

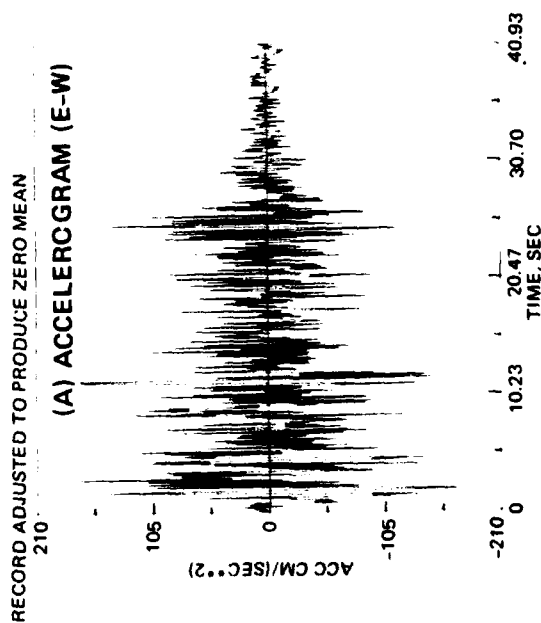
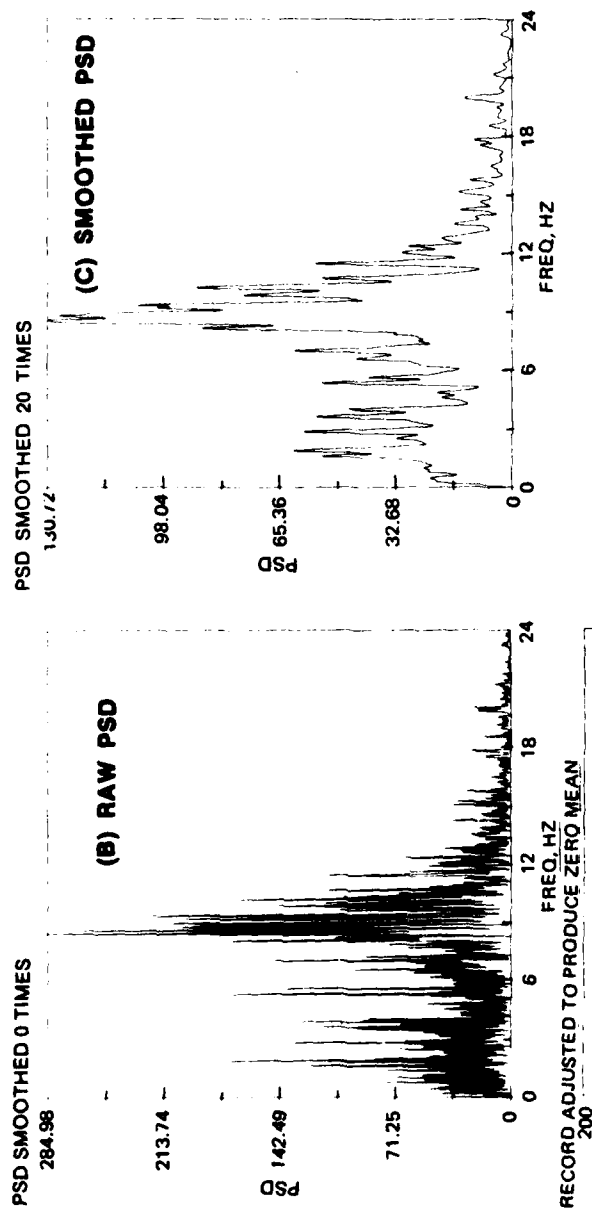


Figure 2. (Sheet 2 of 3)

b.



IMPERIAL VALLEY EARTHQUAKE  
MAY 18, 1940 - 2037 PST  
STATION NO. 117 COMP VERT

C.

Figure 2. (Sheet 3 of 3)

divided by the area  $\lambda^2$  under the power density versus frequency curve. This area may also be called the spectral intensity.

#### Spectral Frequency Range

21. Figures 2a, b, and c show the PSD spectra of N-S, E-W, and vertical components, respectively, of the El Centro earthquake of 18 May 1940. The frequency range shown is between 0 and 24 Hz. While the energy of the PSD in the vertical component spreads between 0 and 22 Hz, the energy of the PSD for the two horizontal components is concentrated in the range of 0 to 10 Hz. For this record, the PSD frequency range of 0 to 10 Hz is adequate for the description of the spectra of the horizontal components.

#### Computer Procedures for Generating PSD

22. The computer program used to calculate one-sided PSD function was provided by Professor M. Shinozuka, Columbia University, and modified for the Honeywell 635 Computer by the U. S. Army Engineer Waterways Experiment Station Automatic Data Processing (WES ADP) Center. The procedures for generating PSD are as follows:

- a. Read in accelerogram.
- b. Scale accelerogram\* so that accelerations are in centimetres per second squared.
- c. Adjust accelerogram\* by interpolation so that the  $\Delta t$  between time points is 0.02 sec.
- d. Extend accelerogram to  $(2^{13} - 1) \times 0.02 = 163.82$  sec by adding trailing zeros to the acceleration record (so far, no accelerogram is longer than 163.82 sec).
- e. Calculate the statistics (mean, standard deviation, etc.) for the extended accelerogram and adjust it to a zero mean.
- f. Calculate the PSD of the extended, zero-mean accelerogram (up to a frequency of 10 Hz).

---

\* If necessary.

- g. Calculate the area under the PSD curve and normalize the curve (NPSD) (i.e., divide each point of the PSD by the area under the PSD curve).
- h. Smooth the PSD curve or NPSD curve using the "Hanning" process.



#### PART IV: DATA PRESENTATION

23. A total of 421 horizontal accelerograms were used to estimate the raw power spectral density (RPSD) function and its variance or RPSD intensity. These calculated PSD functions, normalized to unit area, will be used to represent the frequency content and characteristics of ground motions. The final mean normalized PSD (MNPSD) and MNPSD plus one standard deviation curves for four site groups were plotted.

24. Depending on their recording site conditions, the 421 horizontal records were grouped in Tables 1 to 4:

Table 1 - 56 records for rock sites

Table 2 - 131 records for stiff soil sites

Table 3 - 120 records for deep cohesionless soil sites

Table 4 - 114 records for soft to medium clay and sand

The headings for Columns 1-9 in each table are self-explanatory. The duration in Column 10 is arbitrarily estimated. Column 11 gives the base PSD average power  $\lambda^2$  (note that  $\lambda^2 = I_0/164$ ), which is the area under the RPSD function curve for an extended record length of 163.82 sec, or 164 sec for simplicity. Column 12 gives  $\lambda$ , the average acceleration, or the square root of the corresponding value in Column 11. Column 13 is the factor for conversion of  $\lambda^2$  (Column 11) to  $\lambda_o^2$ , the area under the PSD function for the actual record length (Column 14). This conversion factor in Column 13 is the ratio of the extended time of 163.82 sec to the time of the total record length  $t_o$  or the arbitrarily selected duration (Column 10); i.e., Column 11  $\times$  Column 13 = Column 14, which is the raw average power  $\lambda_o^2$ . Column 15 gives  $\lambda_o$ , the average acceleration for the corresponding Column 14. Column 16 equals Column 14 multiplied by 0.875 and is the final corrected area, or average power  $\lambda_s^2$  under the RPSD function curve. The constant 0.875 is the amount by which the power spectrum estimates should be multiplied so as to obtain the correct scale factor. An explanation for this correction is presented by Bendat and Piersol (1971, p. 323). Column 17 gives the average acceleration  $\lambda_s$  or the square root of the area under the estimated PSD function curve. Actually, the difference between  $\lambda_o$  and

$\lambda_s$  is very small, so it can be considered that  $\lambda_o \approx \lambda_s$ . For practical purposes, the raw average power  $\lambda_o^2$  may be accepted as the scaling factor for the standard (mean or mean plus one standard deviation) NPSD spectrum.

25. Most of the records used in this study were obtained at sites in the western part of the United States or Japan. A few other significant strong-motion records, such as those of the Koyna, India (1967), Gazli, USSR (1976), and Bucharest, Rumania (1977) earthquakes, were also included.

26. The RPSD average power values of the horizontal components for the earthquake accelerograms of El Centro (1934 and 1940), Taft (1952), and Olympia (1949) have been calculated for durations of 25 or 30 sec as indicated in Table 5. The average power of uncorrected versions of these records (for the same durations) was calculated by Ravara (1965) and should be different from that calculated in this study. For the purpose of comparison and evaluation of accuracy, Ravara's values are also listed in Row 1. The numerical values in Row 2 are directly calculated from the CIT corrected records. Average power values adjusted from these calculations for a duration of 163.82 sec to the lengths of the particular records are shown in Row 3. In comparing the average power in Row 2 and Row 4 of Table 5, there is a close agreement. The average power values in Row 3 estimated from the base average power  $\lambda^2$  are higher than those in Row 2, which were directly calculated from the actual (shorter) duration records. Thus, the amount of increased average power (~ a constant factor) caused by adding zeros indicates that the final correction is needed.

27. Table 5 also shows that the average power estimated from the baseline uncorrected accelerograms by Ravara (1965) could have 18 to 66 percent error in comparison with CIT corrected data. The error for the extended 163.82-sec record duration in this study is in the range of 8 to 16 percent. The average error is about 12 percent, which is in agreement with the correction factor of 0.875 (Bendat and Piersol 1971). After the correction factor of 0.875 is applied, the error is reduced from 0.3 to 5.5 percent.

28. In conclusion, the base average power  $\lambda^2$  of 421 records grouped in Column 11 of Tables 1-4, which are presented in a convenient way, can be employed to estimate the average power for any strong-motion duration of an individual accelerogram in the lists of all four tables as long as the selected duration is less than 163.82 seconds. Fortunately, not one of the 421 records exceeds the duration of 163.82 seconds.

29. Table 6 is a comparison of average power calculated by the method of Vanmarcke and Lai (1977) and Vanmarcke (1979) and the method of this study with the same strong-motion durations corresponding to the same records. By comparison of the average power  $\lambda_o^2$  and the average acceleration  $\lambda_o$  for the same record in Table 6, it follows that the values calculated by Vanmarcke and Lai (1977) and in this study are in excellent agreement, even though Vanmarcke and Lai's values of  $\lambda_o^2$  were directly derived from the time domain and the values in this study are calculated in the frequency domain. This comparison is verifying not only the processing techniques but also the theoretical background.

## PART V: DATA ANALYSES

### Analysis of Site-Dependent PSD Spectral Shape

30. The NPSD functions for the horizontal accelerograms in each group (Table 1-4) were first determined and then were analyzed statistically to obtain the average NPSD spectra and the average plus one standard deviation NPSD spectra (about 84 percentile). Figures 3-6 present these mean and mean plus one standard deviation NPSD spectra for the four different site conditions. The mean NPSD spectra for the different site conditions are compared in Figure 7, and the mean plus one standard deviation NPSD spectra are compared in Figure 8. Both NPSD spectra in Figures 7 and 8 are smoothed 500 times.

31. It is clear that the differences in PSD spectral shapes depend on the site conditions. In particular, two categories can be distinguished: sites having soft to medium clays and sands or deep cohesionless soils (>250 ft) are similar and form one category, the soft group; stiff soil and rock sites form another category, the hard group. A dividing line on the frequency axis appears at 2.5 Hz (0.4-sec period). In the frequency range below 2.5 Hz, spectral amplifications for the soft group are much higher than those for the hard group; in the frequency range above 2.5 Hz, spectral amplifications for the hard group are higher than those for the soft group. In the soft group, the energy peaks for the soft to medium clays and sands and the deep cohesionless soils both occur at about the same frequency of 1 Hz, but the amplifications are slightly different (0.4 and 0.35, respectively).

32. The average NPSD spectrum of the deep cohesionless soil sites has a large hump at 2.8 Hz (0.36-sec period), but the spectrum of the soft to medium clay and sand sites does not. The large amplitude at 0 Hz is believed to be caused by a digitization error, particularly that due to the uncorrected Japanese strong-motion data in the soil site group. For the hard site group, in the frequency range below 2.5 Hz, the spectral amplitude for the stiff soil is higher than that for the rock; but in the frequency range above 2.5 Hz, the spectral amplitude

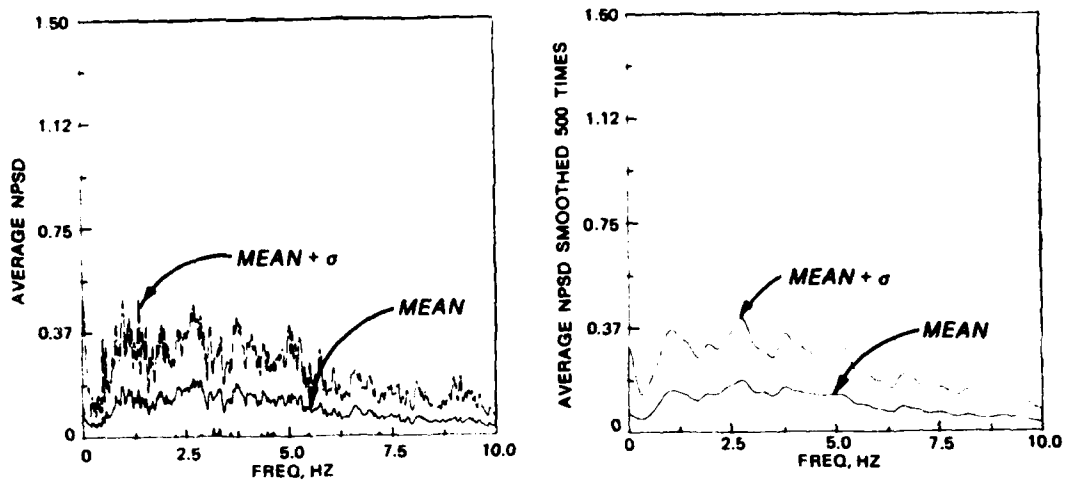


Figure 3. Mean and mean plus one standard deviation ( $\sigma$ ) NPSD curves of rock sites, raw (left) and smoothed 500 times (right)

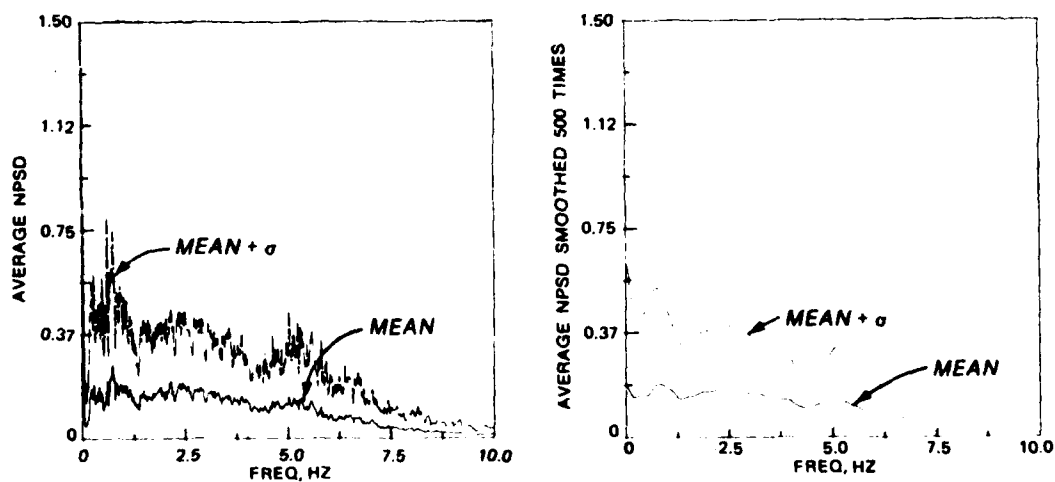


Figure 4. Mean and mean plus one standard deviation ( $\sigma$ ) NPSD curves of stiff soil sites, raw (left) and smoothed 500 times (right)

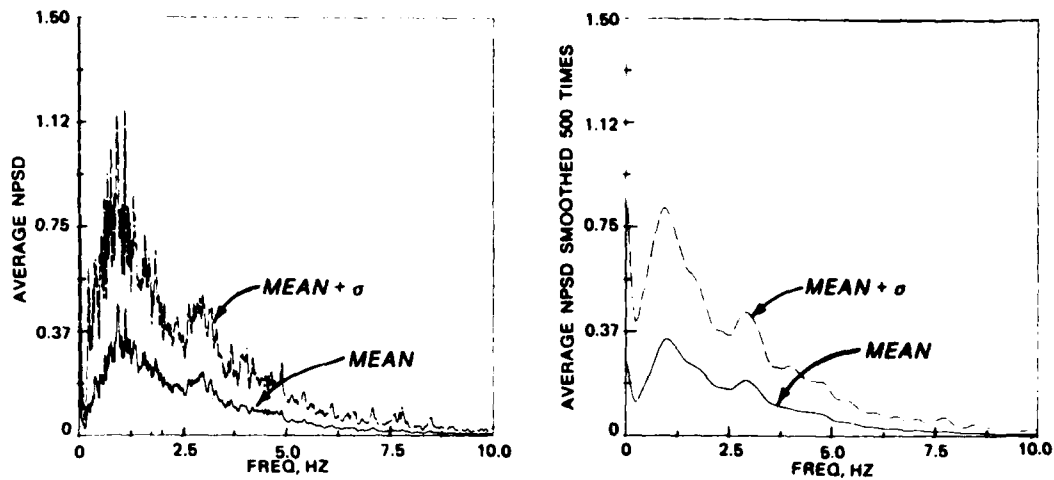


Figure 5. Mean and mean plus one standard deviation ( $\sigma$ ) NPSD curves of deep cohesionless soil sites, raw (left) and smoothed 500 times (right)

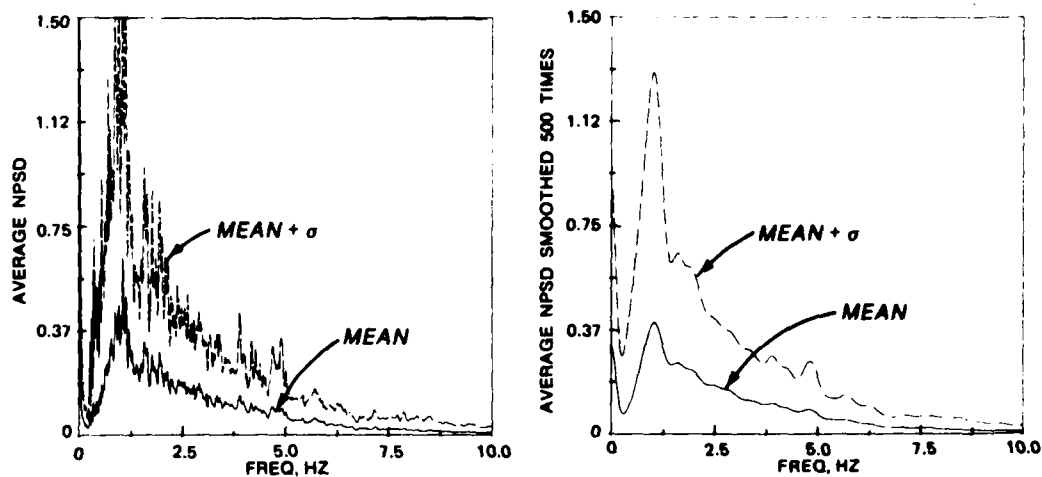


Figure 6. Mean and mean plus one standard deviation ( $\sigma$ ) NPSD curves of soft to medium clay and sand sites, raw (left) and smoothed 500 times (right)

# LEGEND

- GROUP 1 ROCK SITES (56 RECORDS, 11 EARTHQUAKES)
- GROUP 2 STIFF SOIL SITES (131 RECORDS, 39 EARTHQUAKES)
- GROUP 3 DEEP COHESIONLESS SOIL SITES (120 RECORDS, 47 EARTHQUAKES)
- GROUP 4 SOFT TO MEDIUM CLAY AND SAND SITES (114 RECORDS, 28 EARTHQUAKES)

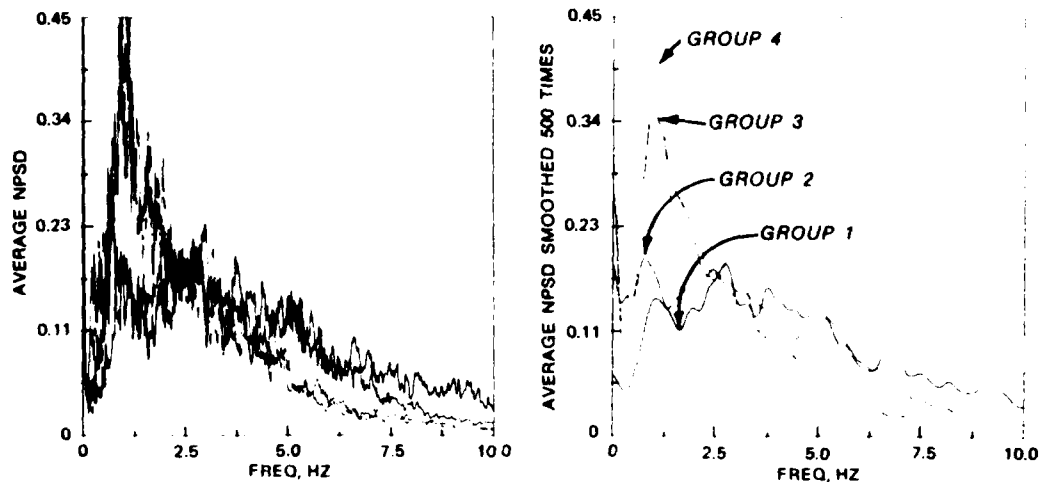


Figure 7. Comparison of mean NPSD curves of four soil groups, raw (left) and smoothed 500 times (right)

# LEGEND

- GROUP 1 ROCK SITES (56 RECORDS, 11 EARTHQUAKES)
- GROUP 2 STIFF SOIL SITES (131 RECORDS, 39 EARTHQUAKES)
- GROUP 3 DEEP COHESIONLESS SOIL SITES (120 RECORDS, 47 EARTHQUAKES)
- GROUP 4 SOFT TO MEDIUM CLAY AND SAND SITES (114 RECORDS, 28 EARTHQUAKES)

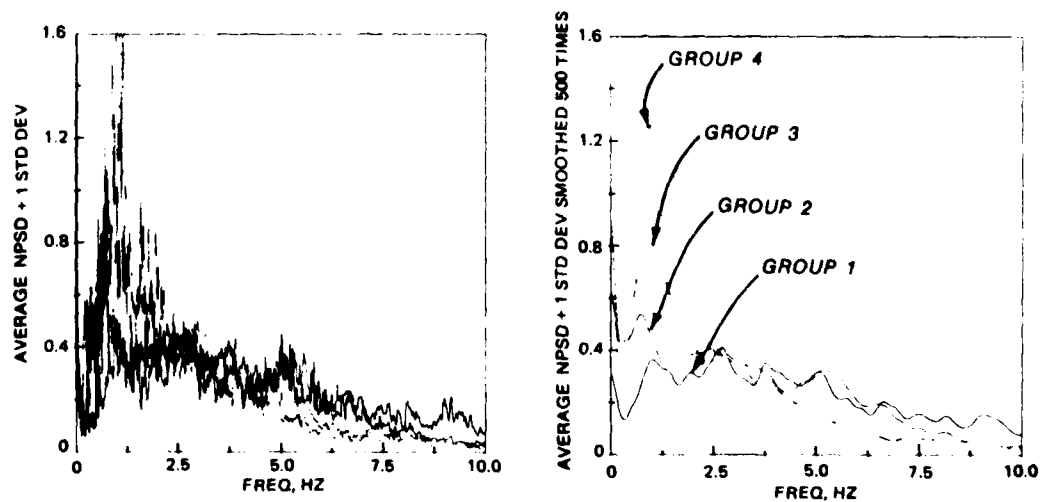


Figure 8. Comparison of mean plus one standard deviation NPSD curves of four soil groups, raw (left) and smoothed 500 times (right)

for the rock is slightly higher than that for the stiff soil. The largest energy peaks for the rock sites and the stiff soil sites are at 2.75 Hz (0.36 sec) and 0.8 Hz (1.25 sec), respectively.

#### Statistical Characteristics of the Earthquake Ground Motions

33. Based on the maximum ground accelerations and average accelerations (PSD intensities) in Tables 1-4, and the average NPSD function estimates for the four site conditions (Figures 7 and 8), Table 7 lists the statistical characteristics of the earthquake ground motions.

34. It is apparent from Table 7 that statistical characteristics of the ground motions are strongly site dependent. The rock sites produce an average maximum ground acceleration of about 0.20 g for the entire suite of 56 records. The rock site group shows the highest maximum acceleration and average acceleration of the four site groups. The PSD function estimates are almost uniform over the peak frequencies of 1.06, 2.75, 3.80, and 5.17 Hz.

35. The average maximum ground accelerations and PSD spectral intensities (or average accelerations) for the other three site groups--stiff soils, deep cohesionless soils, and soft to medium clays and sands--are relatively close together. However, the spreads of the standard deviation of maximum accelerations for the stiff soil and cohesionless soil groups are wider than for the soft to medium clays and sands group. This large spread is believed to be caused by the different magnitudes of earthquakes and the different epicentral distances. The group of accelerograms for soft to medium clays and sands shows relatively low ground acceleration but the highest PSD function estimates at the frequency of 1 Hz among the four groups. One second (1 Hz) is probably near the predominant natural period of sites on soft to medium clays and sands. It seems that the acceleration and the PSD spectral intensity at 1 Hz are roughly in proportion and inverse proportion, respectively, to the degree of stiffness of the site material. In conclusion, the average acceleration or the mean spectral intensity is site dependent.



### Maximum Ground Acceleration and Average Acceleration

36. Figures 9-16 show plots of maximum ground accelerations  $a_{\max}$  against base average accelerations  $\lambda$  (i.e., the rms value of the average power for extended durations of 163.82 sec) and against the average acceleration  $\lambda_s$  (for selected or actual record durations) for each of the four site condition groups. These figures indicate a common linear trend for all four groups. This approximately linear relationship may provide a basis for predicting strong earthquake ground motions for engineering design. The data points show greater scatter on the plots of  $a_{\max}$  versus  $\lambda$  than on the plots of  $a_{\max}$  versus  $\lambda_s$ . However, mean lines for both kinds of plot are parallel, probably because of the close relationship between  $\lambda$  and  $\lambda_s$ . Also, the data points for soft sites show a wider spread than those for hard sites.

36. It is worthwhile to note that there is a strong correlation (Figures 17 and 18) between  $a_{\max}$  and  $\lambda_o$ , which were derived from the values of  $I_o = S_o \lambda_o^2$  of 140 strong-motion records in Vanmarcke and Lai (1977, 1980). The quantity  $I_o$  is the total motion energy at constant power  $\lambda_o^2$  over the strong-motion duration  $S_o$ . Twenty-two of the 140 records are for rock sites, and the rest are for soil sites. At the same time, the two mean lines for rock sites and soil sites are almost identical, thus indicating that the linear relationship between  $a_{\max}$  and  $\lambda_o$  is independent of the site conditions. The mean lines of  $a_{\max}$  versus  $\lambda_o$  calculated from the strong-motion data of Vanmarcke and Lai (1977) are also plotted in Figures 10, 12, 14, and 16 and lie to the right of the data for this study. Since  $\lambda_o$  is inversely proportional to  $S_o$ ,  $\lambda_o$  is minimum when the whole record length is considered. The durations selected in this study were close to the whole record lengths; thus, the calculated average accelerations are lower than the rms accelerations of Vanmarcke and Lai (1977).

### Peak Factor

38. The peak factor  $r$  is defined as the ratio of the peak

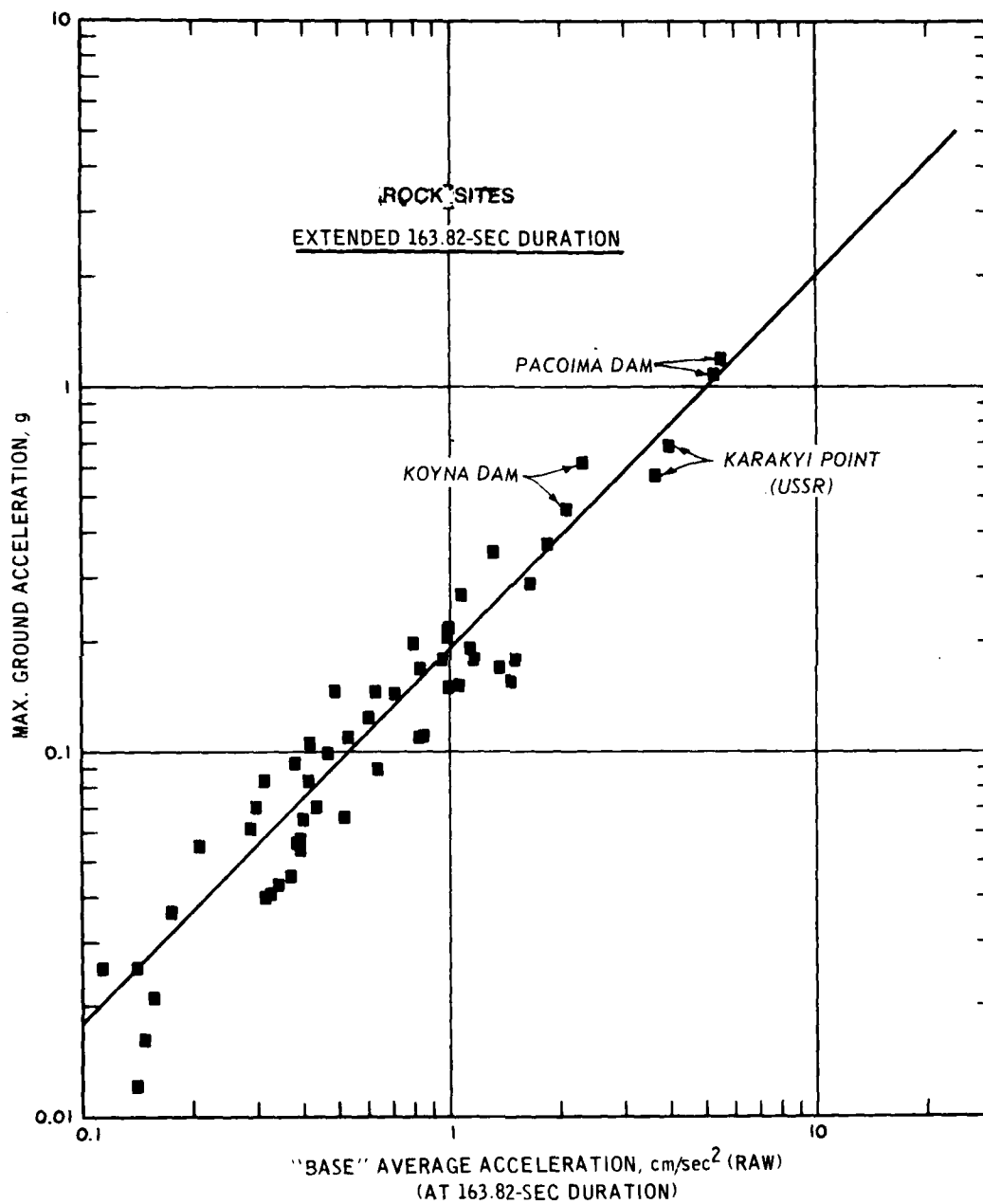


Figure 9. Correlation of maximum ground acceleration (g) versus "base" average acceleration calculated based on extended 163.82-sec duration for rock sites

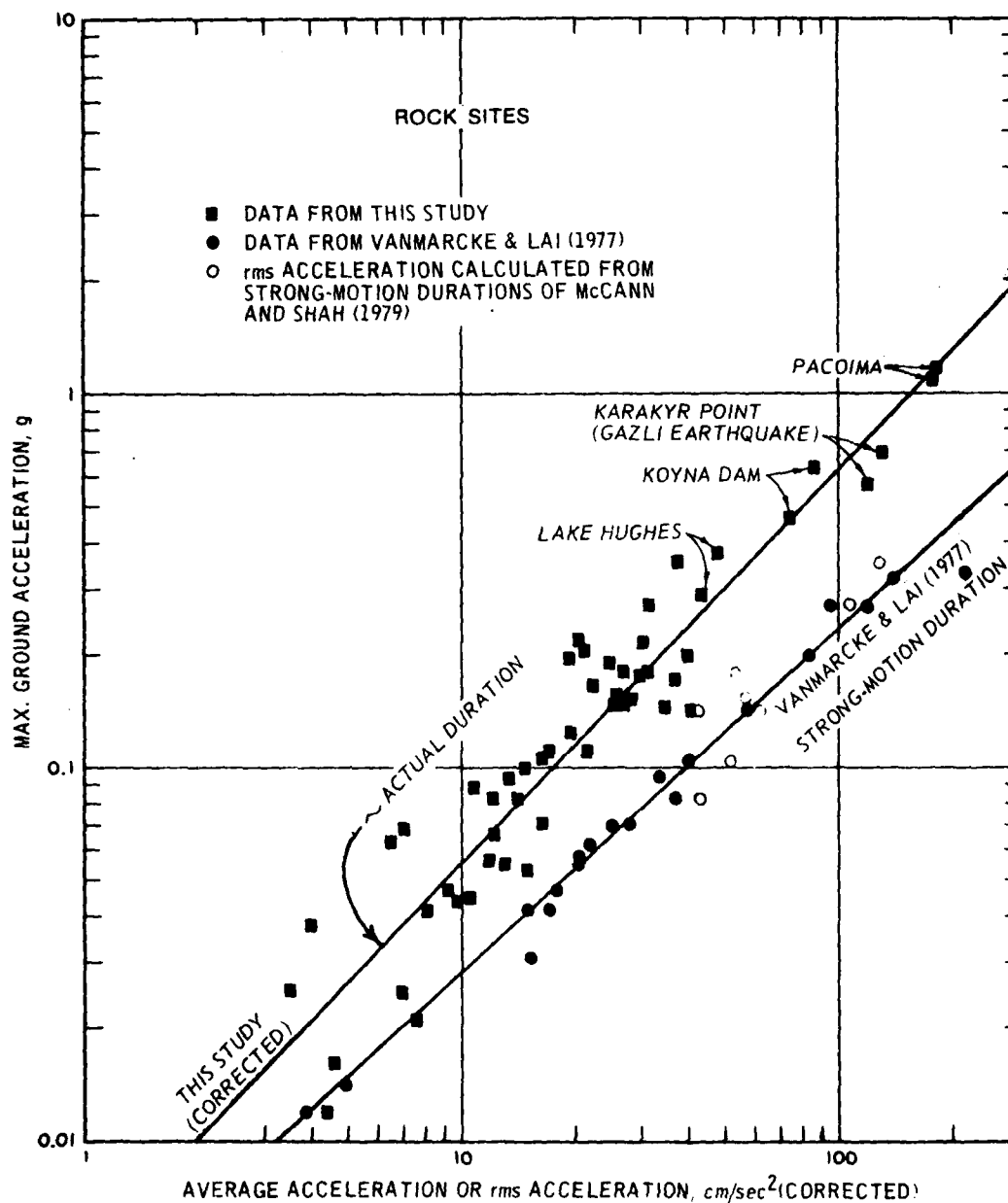


Figure 10. Correlation of maximum ground acceleration (g) versus average acceleration and rms acceleration based on actual durations and strong-motion durations for rock sites

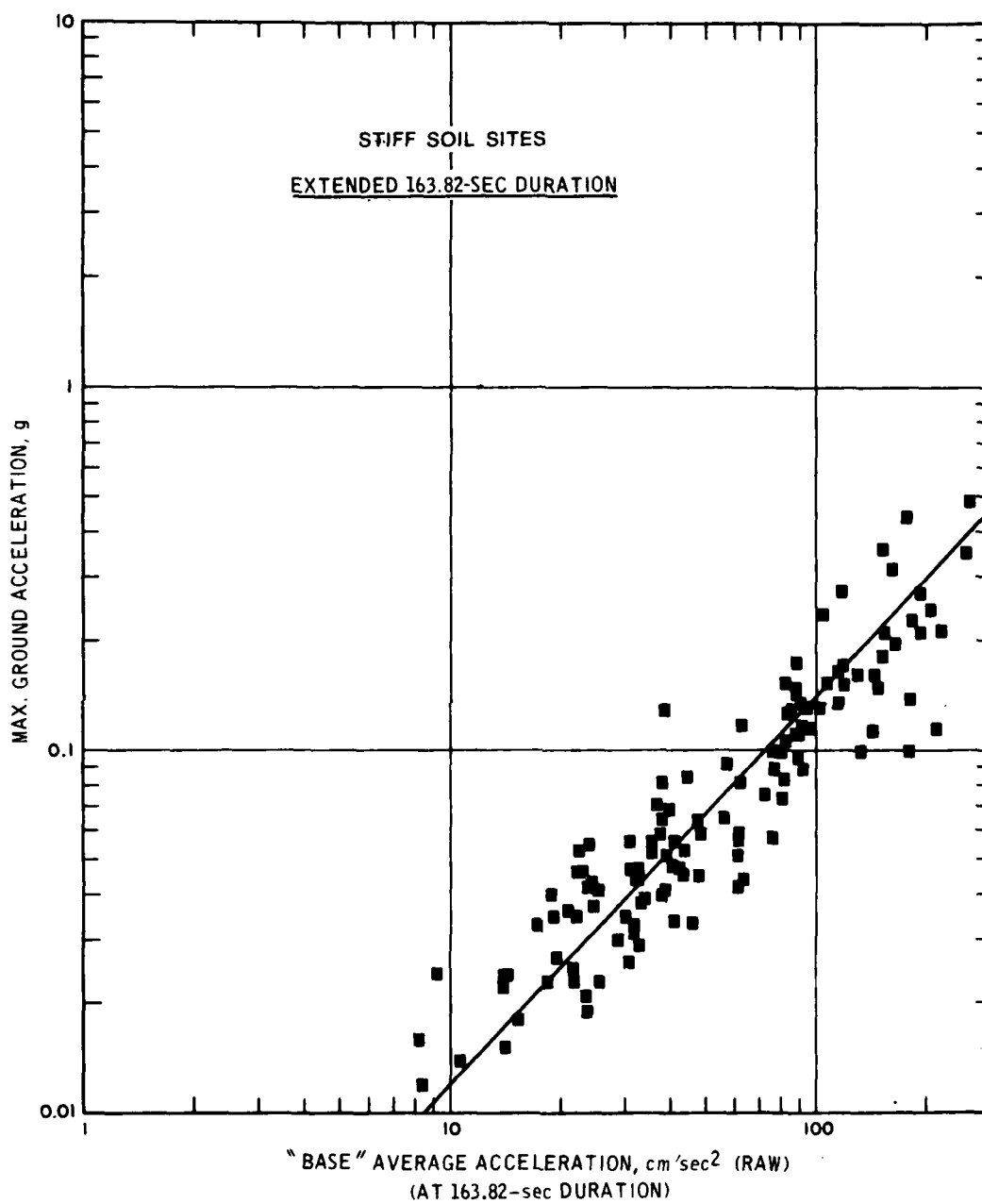


Figure 11. Correlation of maximum ground acceleration (g) versus "base" average acceleration based on extended 163.82-sec duration for stiff soil sites

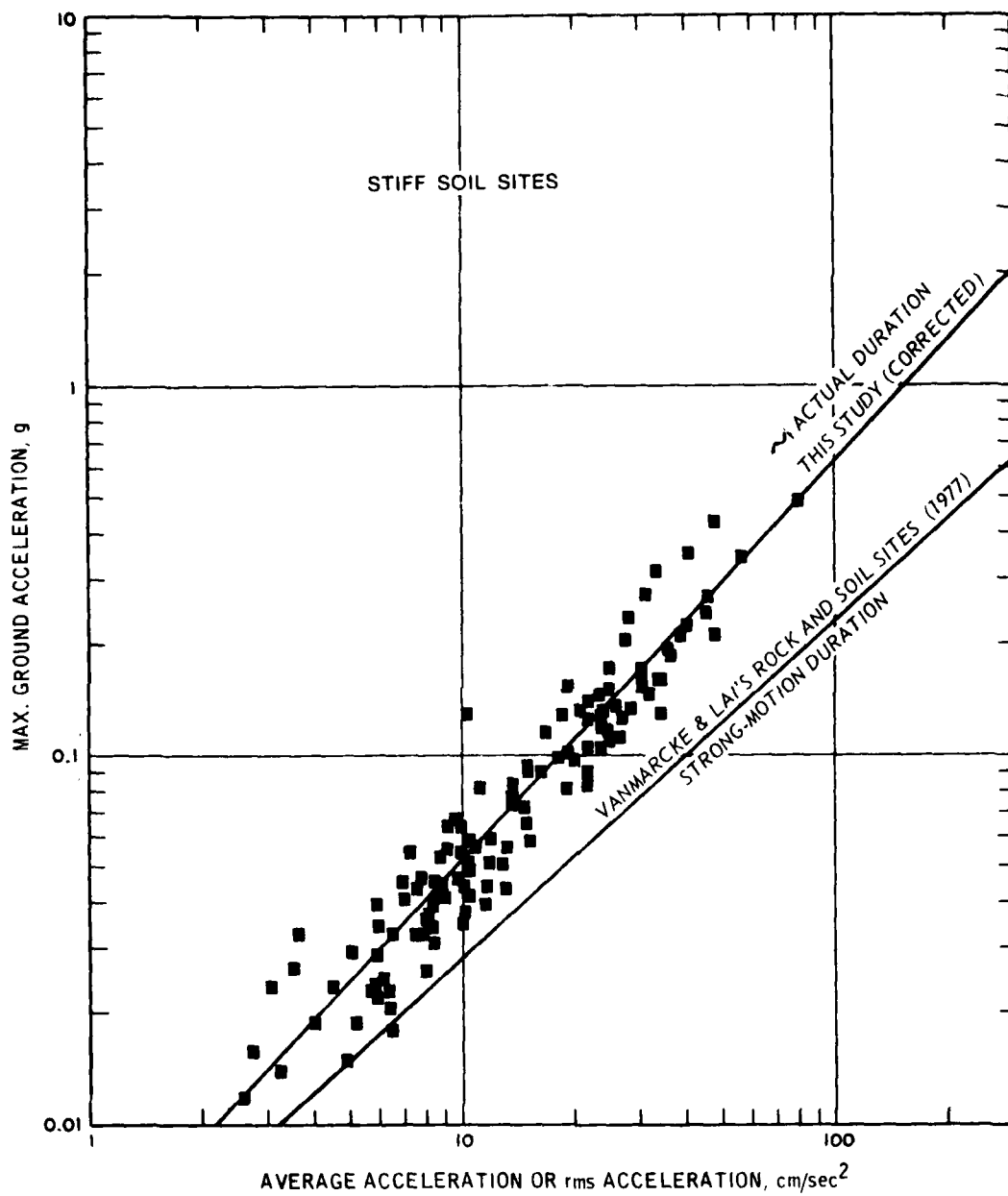


Figure 12. Correlation of maximum ground acceleration (g) versus average accelerations and rms accelerations based on actual durations and strong-motion durations for stiff soil sites

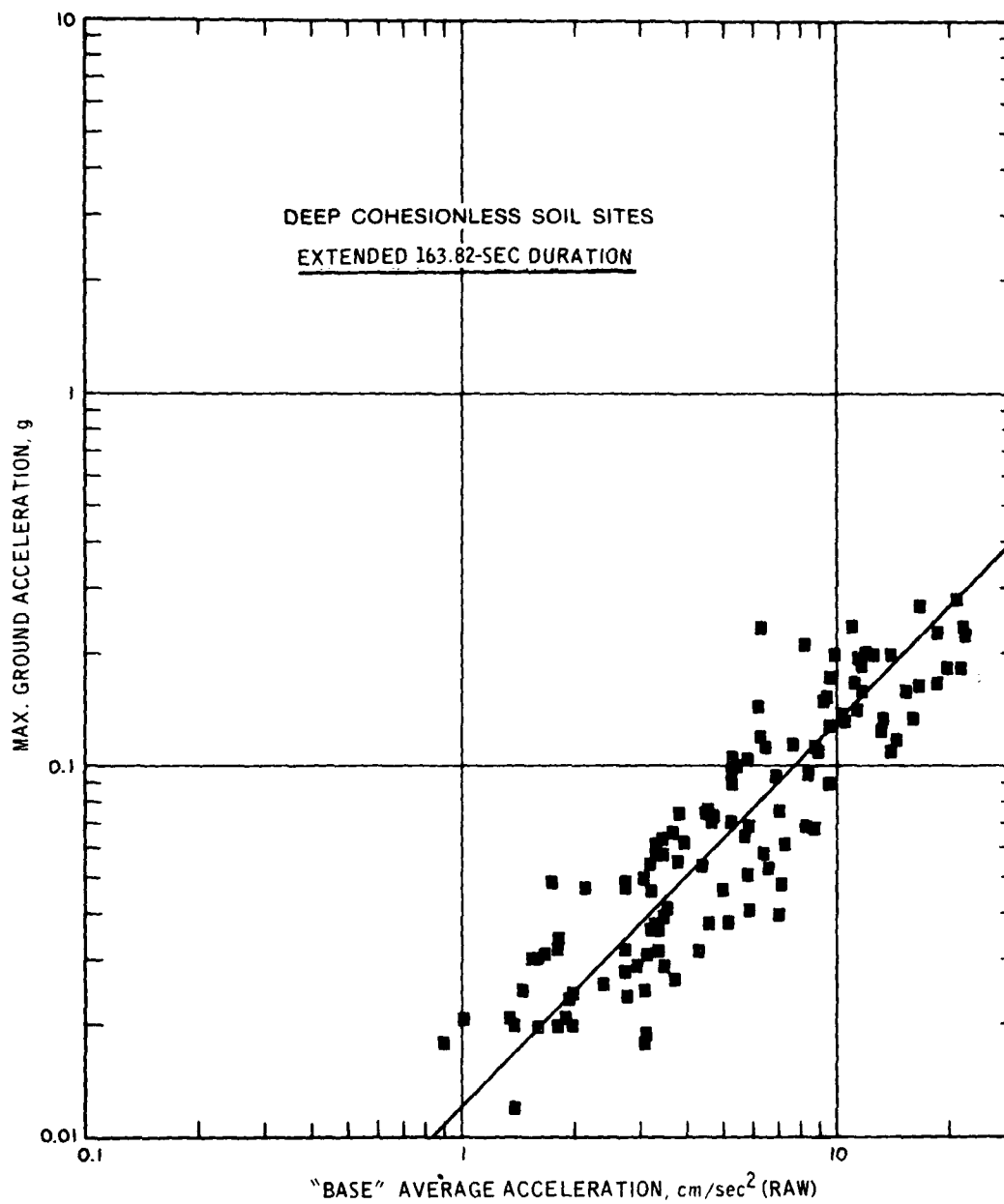


Figure 13. Correlation of maximum ground acceleration (g) versus "base" average acceleration based on extended 163.82-sec duration for deep cohesionless soil sites

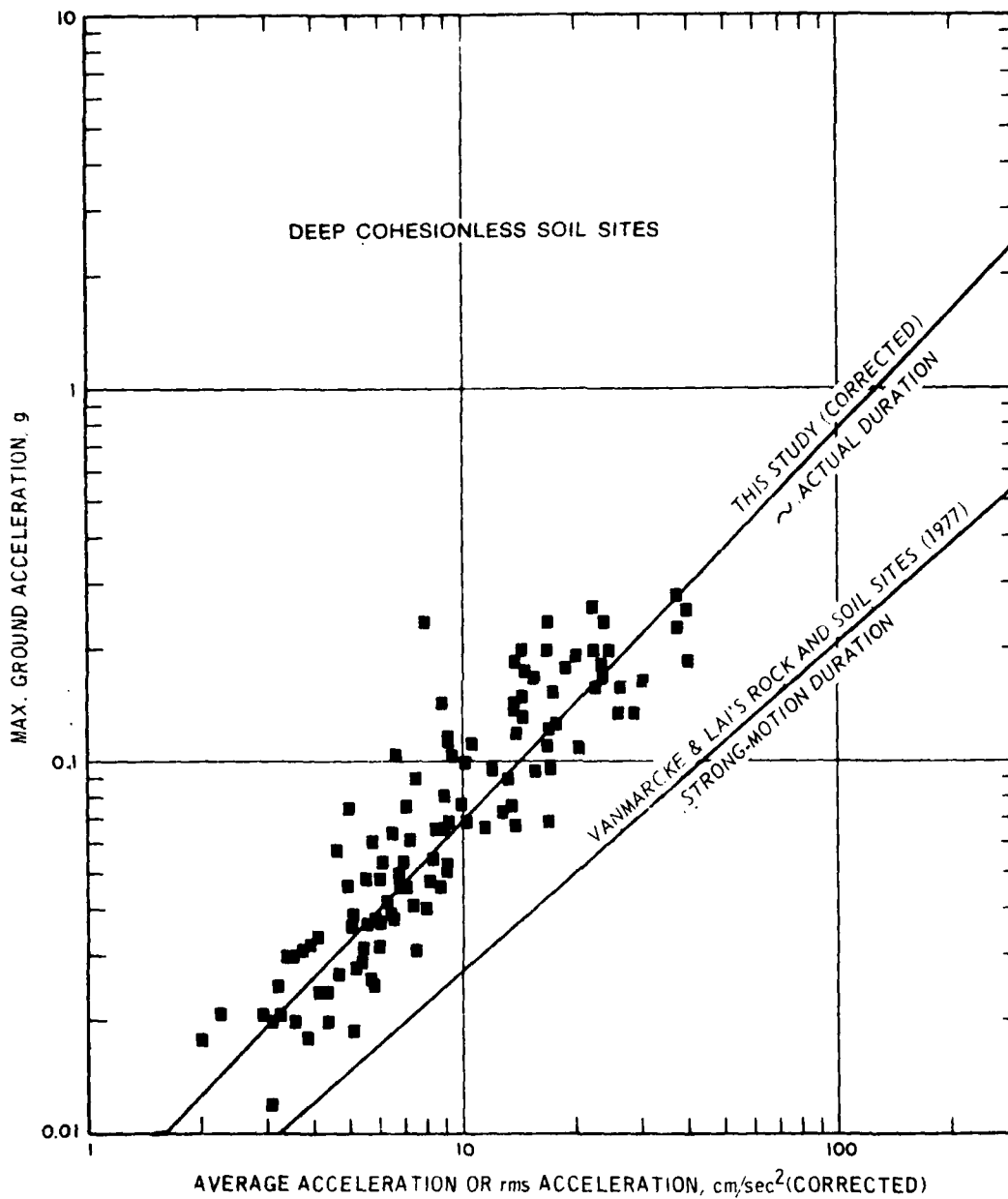


Figure 14. Correlation of maximum ground acceleration (g) versus average acceleration and rms acceleration based on selected actual durations and strong-motion durations for deep cohesionless soil sites

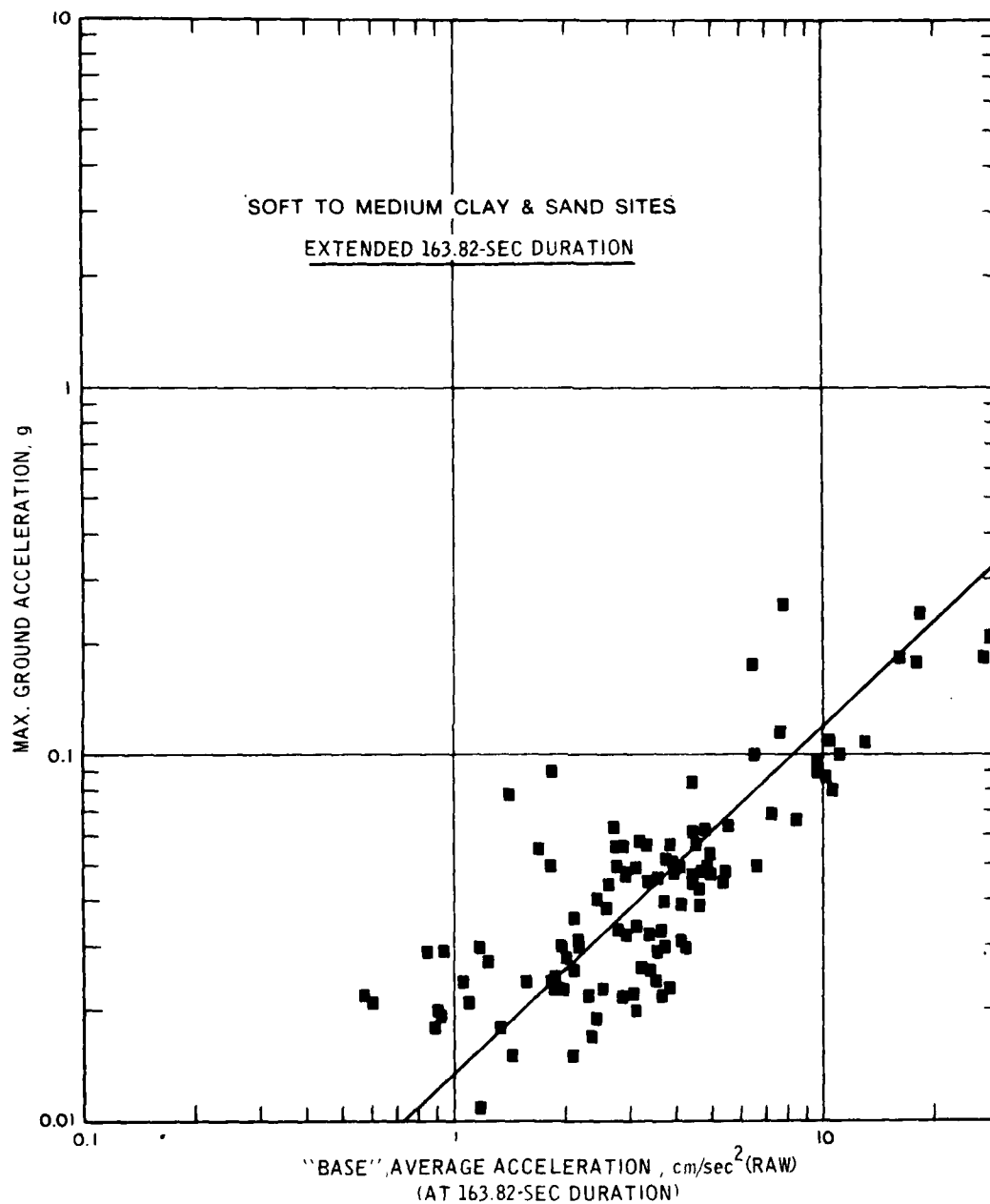


Figure 15. Correlation of maximum ground acceleration (g) versus "base" average acceleration based on extended 163.82-sec duration for soft to medium clay and sand sites



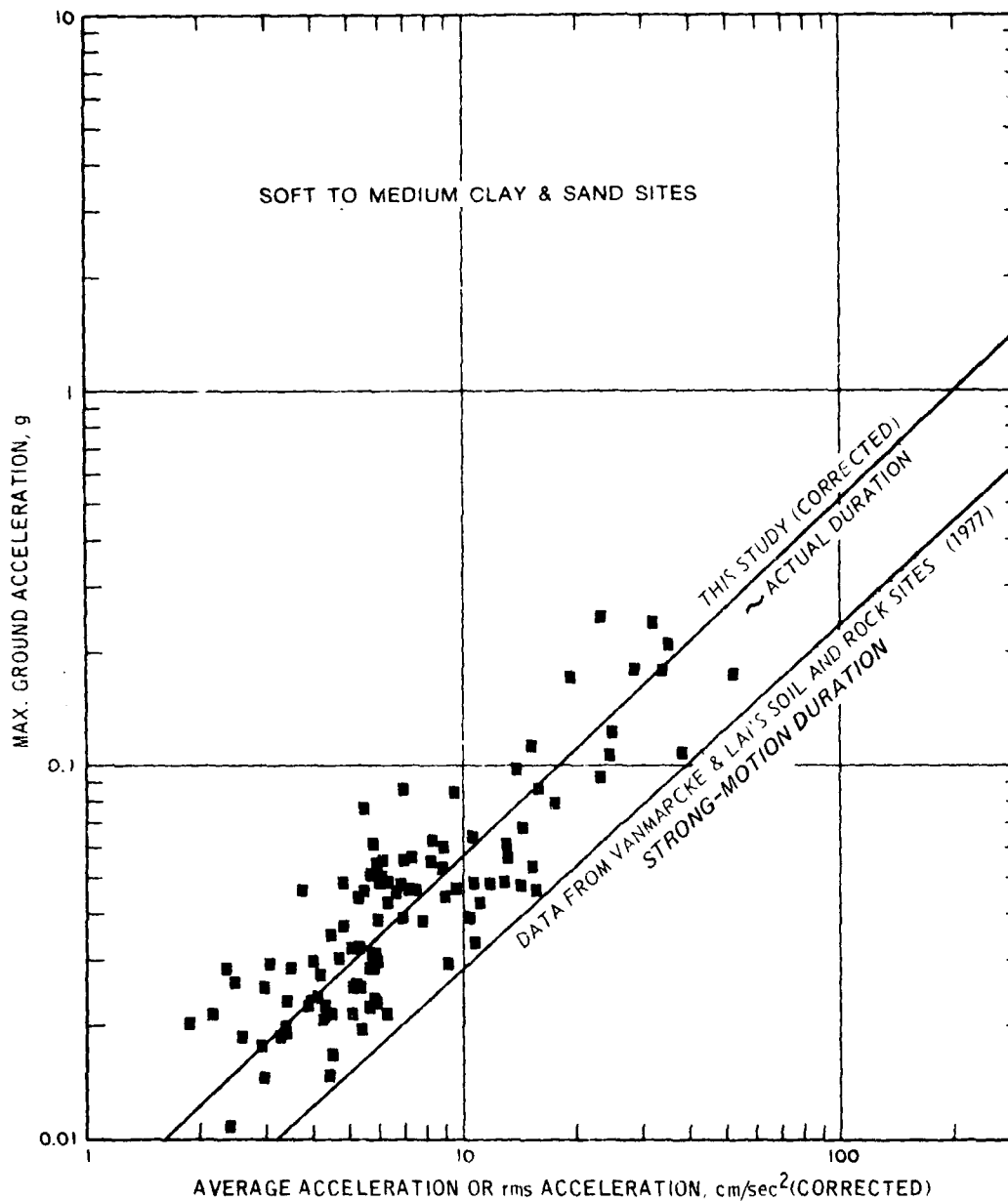


Figure 16. Correlation of maximum ground acceleration (g) versus average acceleration and rms acceleration calculated based on selected actual durations and strong-motion durations for soft to medium clay and sand sites

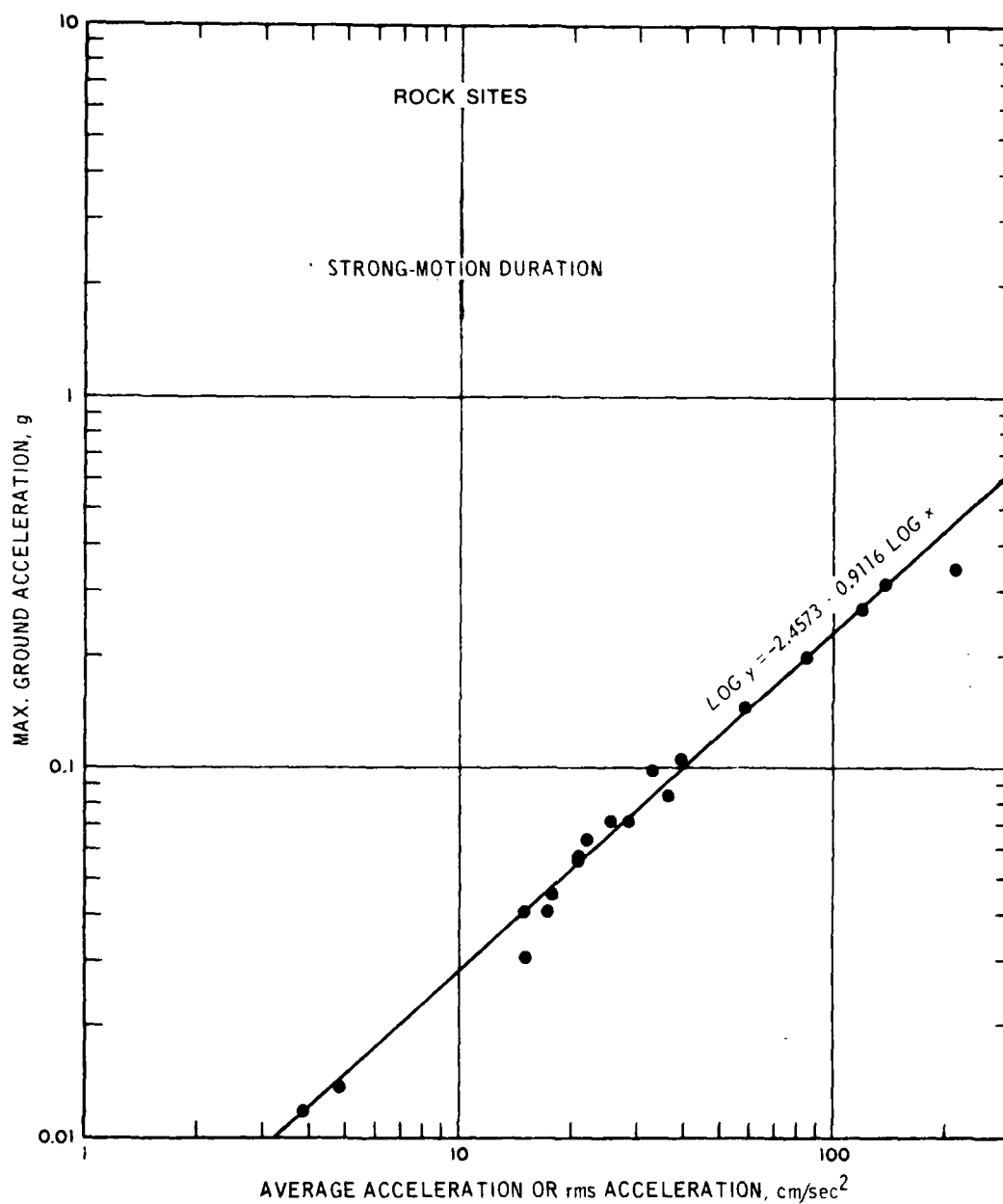


Figure 17. Maximum ground acceleration (g) versus rms or average acceleration for strong-motion duration case - rock sites

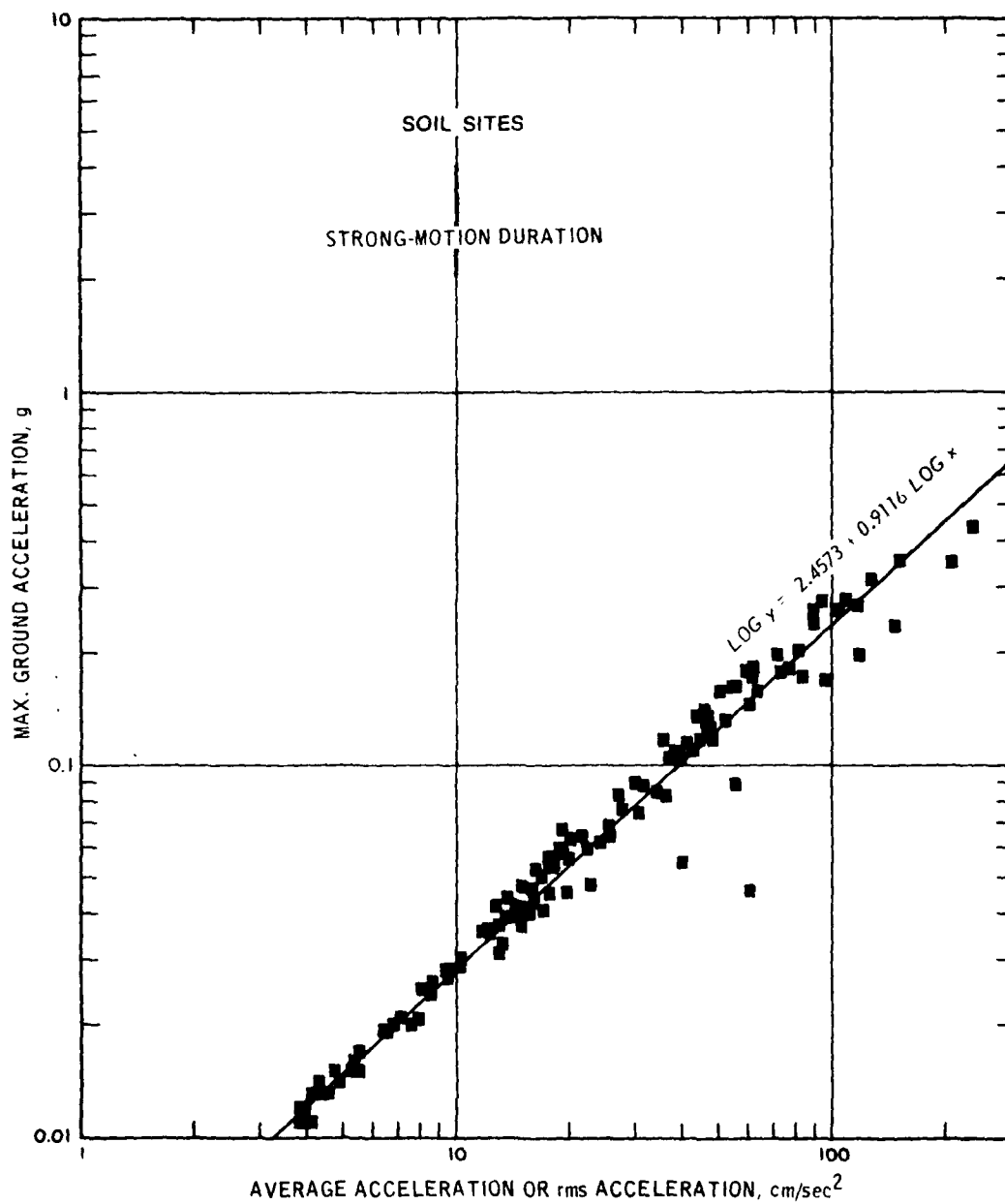


Figure 18. Maximum ground accelerations (g) versus rms or average acceleration for strong-motion duration case - soil sites

ground acceleration  $a_{\max}$  to the average acceleration  $\lambda_o$ , or

$$r = \frac{a_{\max}}{\lambda_o} \quad (22)$$

The physical meaning of  $r$  is the slope of the lines plotted in Figures 9-18. Equation 22 may be written as

$$\lambda_o = \frac{a_{\max}}{r} \quad (23)$$

If Equation 23 is substituted into Equation 16, the result may be expressed as

$$S_o = r^2 \frac{I_o}{2 a_{\max}} \quad (24)$$

where  $r$  is a constant that may be determined from Figures 9 through 16. The average peak factors for rock sites, stiff soil sites, deep cohesionless soil sites, and soft soil sites found in this study were 5.911, 5.422, 6.996, and 5.695, respectively. Evidently, the peak factors are nearly independent of site conditions. Therefore, an average peak factor of 6.0 is an adequate estimate for use with long record lengths such as those used in this report. However,  $r$  is dependent on the choice of record duration. Vanmarcke and Lai (1980) found the average peak factor for 140 horizontal earthquake records to be about 2.75 because they used strong-motion durations. Their simplified definition of strong-motion duration is

$$S_o = (2.75)^2 \frac{I_o}{2 a_{\max}} = 7.5 \frac{I_o}{2 a_{\max}} \quad (25)$$

However, Equation 25 is not employed in this study.

#### Comparison of Average Acceleration and Peak Ground Acceleration Versus Distance

39. The average acceleration  $\lambda_o$  in Tables 1-3 and the peak

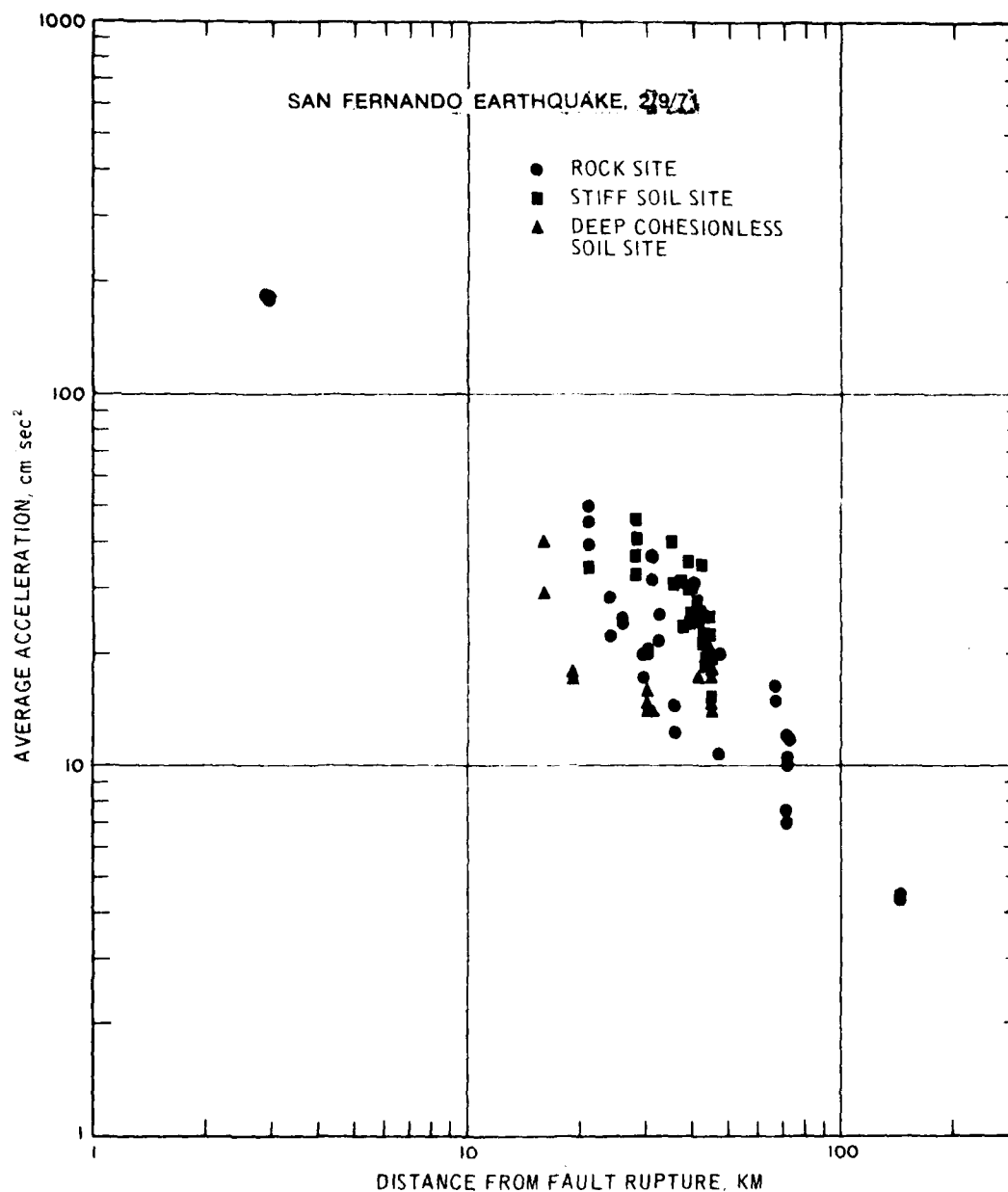
ground acceleration (PGA) or  $a_{\max}$  of the San Fernando earthquake of 9 February 1971 are compared qualitatively in Figures 19 and 20. The spread of the average acceleration is as wide as that of the PGA, but the attenuation of the average acceleration is slower than that of the PGA. The average acceleration of an accelerogram is inversely proportional to the duration, which in this study was arbitrarily selected. In earthquake engineering design, both strong-motion duration and wave amplitude should be considered. The average power of the PSD function and the average acceleration, the square root of the average power, possess information on both duration and amplitude. The previous sections have shown good correlation between the PGA or  $a_{\max}$  and the average acceleration  $\lambda_o$ . The average acceleration can provide an alternative earthquake engineering intensity scale, describe the intensity of ground motion for input to structural design, and also serve to compute the scaling factor  $\lambda_o^2$  of the normalized standard PSD spectra.

#### Potential Uses of Site-Dependent Standard NPSD Spectral Curves

40. In the previous sections of Part V, the four standard site-dependent PSD spectral curves at the common record length of 163.82 sec have been established, and they were also normalized to a unit area. The relationships between the shape of the spectral density function and the duration of strong ground motion for individual records will be explained in an example. It is very easy to select an actual record in Tables 1-4 and to modify its duration only for consistency with a specified design earthquake. Use the N-S component of the El Centro record, 18 May 1940, as an illustration: Record No. 3 of Table 2 shows that the base PSD intensity  $\lambda_o^2$  (average power) for a duration of 163.82 sec is  $663.202 \text{ cm}^2/\text{sec}^4$ . Next, let the specified duration for seismic design be 40 sec, then the new PSD intensity will be

$$\lambda_o^2 = 663.202 \times \frac{163.82}{40} = 2716.1 \text{ cm}^2/\text{sec}^4$$

This value,  $2716.1 \text{ cm}^2/\text{sec}^4$ , is also the scaling factor.





41. An alternative way is to employ the approximate linear relationships between  $a_{\max}$  and  $\lambda$  and between  $a_{\max}$  and  $\lambda_0$  (for the rock site condition, Figures 9 and 10). If 0.30-g maximum ground acceleration and 15-sec duration are chosen as the design ground motion, what will the scaling factor be for the normalized mean PSD curve for rock sites? In Figure 9, the base average acceleration  $\lambda$  for 0.30 g is 15.5 cm/sec<sup>2</sup>, and the conversion factor is 163.82/15 = 10.923; then  $(15.5)^2 \times 10.923 = 2624.25 \text{ cm}^2/\text{sec}^4$  ( $\lambda_0 = 51.22 \text{ cm/sec}^2$ ). Thus, 2624.25 cm<sup>2</sup>/sec<sup>4</sup> is the scaling factor.

#### Peak Velocity Versus Average Acceleration

42. Figure 21 shows the relationship between the peak velocity and the average acceleration. All 140 average acceleration values in this figure were calculated from the total ground motion intensity  $I_0$  listed in the tables of Vanmarcke and Lai (1977) or Vanmarcke (1980), except those of Gazli and Pacoima. All peak velocities are given by Chang (1978). These data points (4.5 < M < 6.8) spread over a wide band; the upper line shown corresponds to magnitude 6.5 and the lower to magnitude 5.5. In the relationship between the peak acceleration and the average acceleration in Figures 17 and 18, this particular feature is not shown, because the velocity is related to the intensity or energy level, and thus magnitude. The largest earthquake represented is the Kern County earthquake of 1952, for which the surface-wave magnitude  $M_s$  was estimated as 7.7. Professors Bolt (1978) and Nuttli et al. (1979) found the local magnitude  $M_L$  and the body-wave magnitude  $M_b$  to be 7.2 and 6.8, respectively. Thus, 6.8 has replaced 7.7 in Figure 21.

43. Vanmarcke and Lai's (1977, 1980) total intensity data were used for calculating average acceleration because they have a unique definition of strong-motion duration. These data were obtained from  $I_0 = S_0 \lambda_0^2$  where  $S_0$  is the strong-motion duration and  $\lambda_0^2$  is the square of average acceleration, or average power.



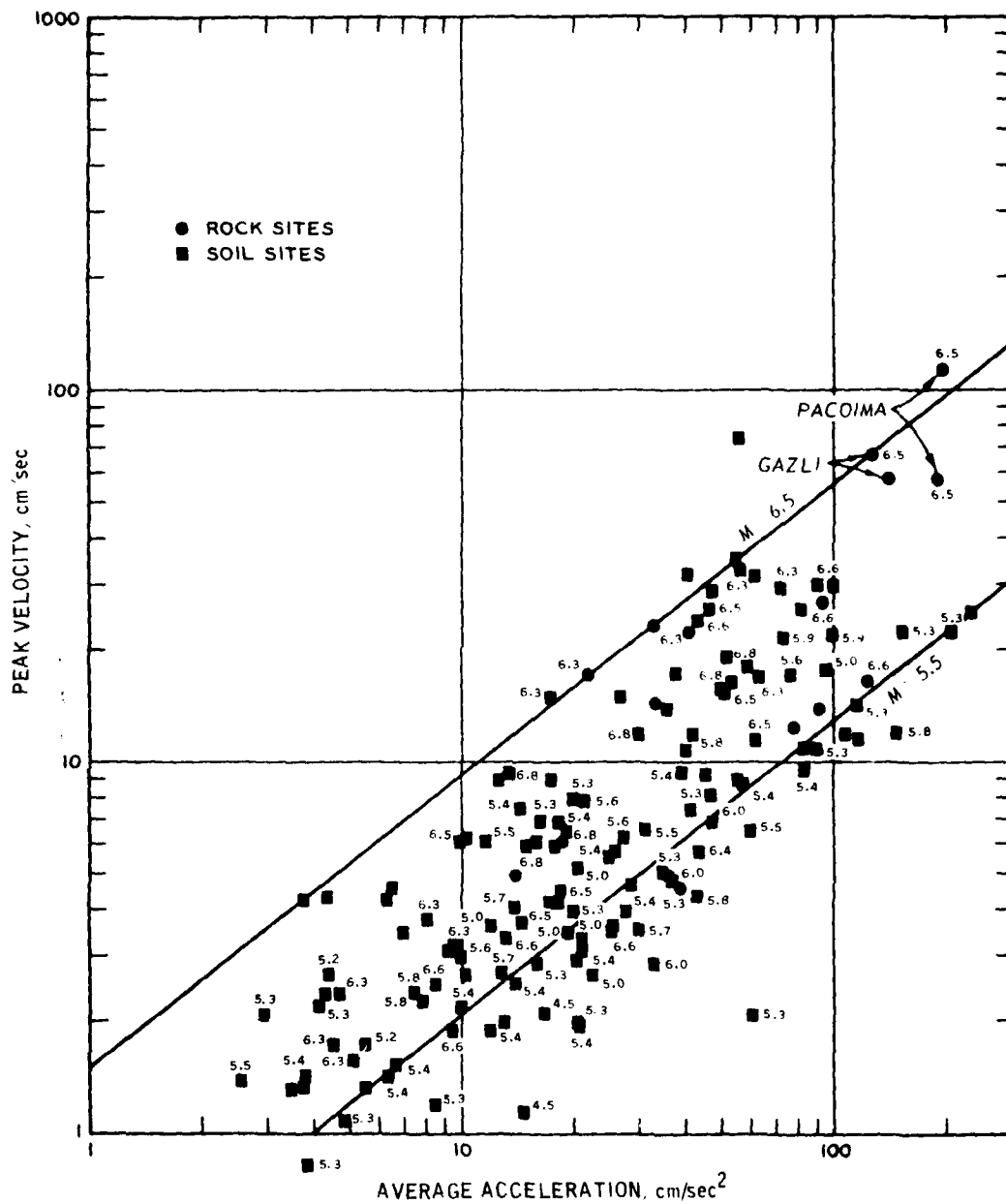


Figure 21. Correlation of peak velocity versus average acceleration

#### Correlation of Average Acceleration and Modified Mercalli Intensity

44. It will be of much benefit to the engineering community if a quantitative earthquake intensity scale, such as average acceleration intensity, can be correlated with the Modified Mercalli Intensity (MMI) (Figures 22 and 23). Table 8 shows the upper bound of site-dependent rms intensity (square root of the sum of two horizontal average powers) versus the MMI. To obtain these bounds in the table, the rock and stiff soil sites in Figure 22 were combined as hard sites and the deep cohesionless soil and soft soil sites in Figure 23 as soft sites. The Pacoima Dam, Karakyr Point, Koyna Dam, and Lake Hughes Array No. 12 sites were located in the epicentral regions and near the faults ( $3\text{km} \leq R \leq 20\text{km}$ ). Certainly, they possessed the maximum average acceleration and might be called epicentral average accelerations. It seems from these limited data that the maximum average acceleration at the epicentral region might not be over  $550.0 \text{ cm/sec}^2$ . However, the power  $\lambda_0^2$  or the average acceleration  $\lambda_0$  is inversely proportional to the duration, i.e., the smaller the duration, the higher the average acceleration.

#### Correlation of $I_0$ and MMI

45. The correlations of total intensity  $I_0$  with the MMI based on the data of hard sites (Tables 1 and 2) and soft sites (Tables 3 and 4), are plotted in Figures 24 and 25, respectively. The upper bound line of Figure 24 is established by five earthquakes (San Fernando, Gazli, Parkfield, Koyna, and Tokachi Oki). There are four sites located in the epicentral region (see paragraph 44), so the values are named as epicentral intensities. The extrapolation from these values, the probable epicentral seismic intensities versus the MMI, may be listed as follows:

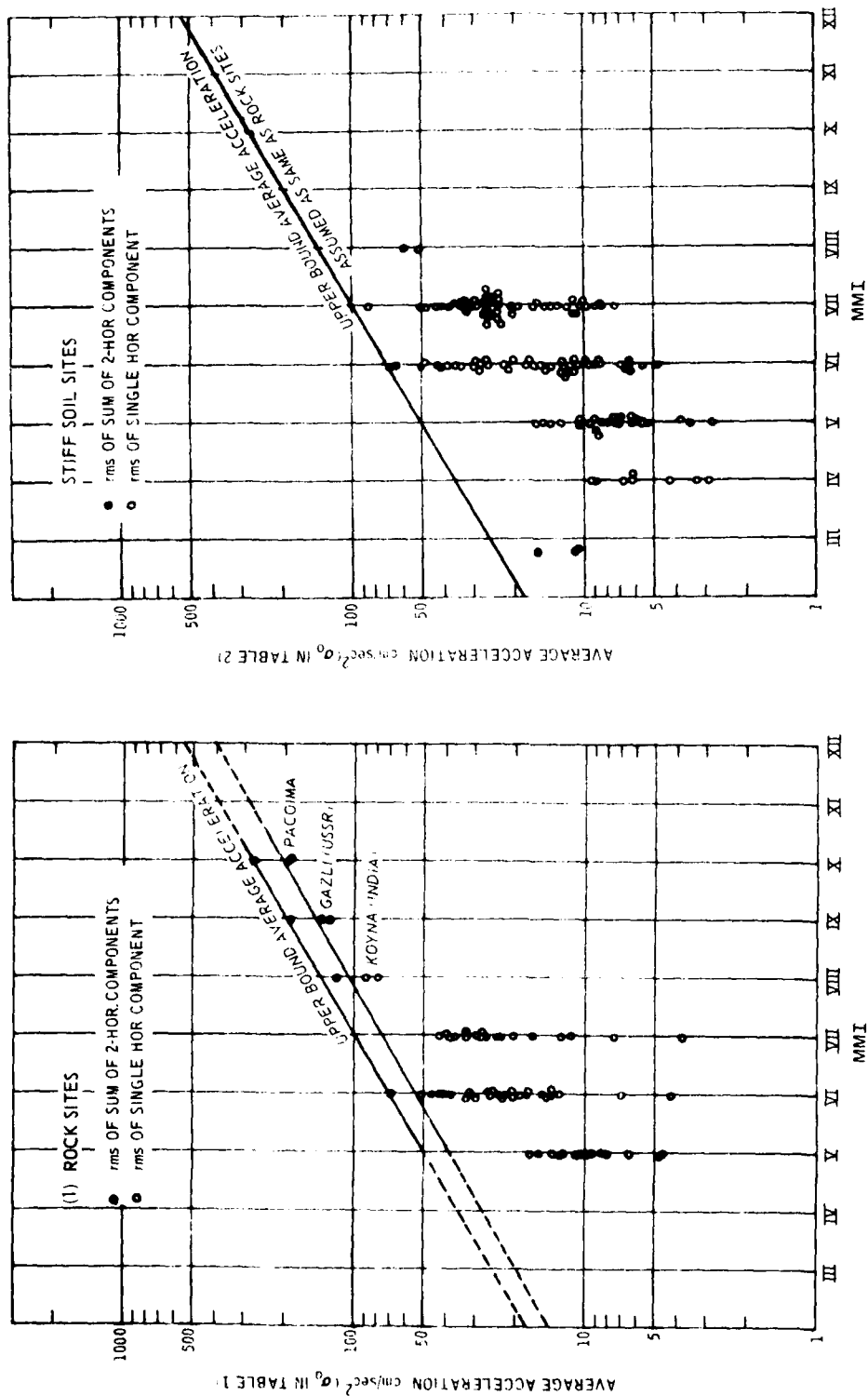


Figure 22. Correlation of upper-bound average acceleration versus MMI - hard sites (rock and stiff soil sites)

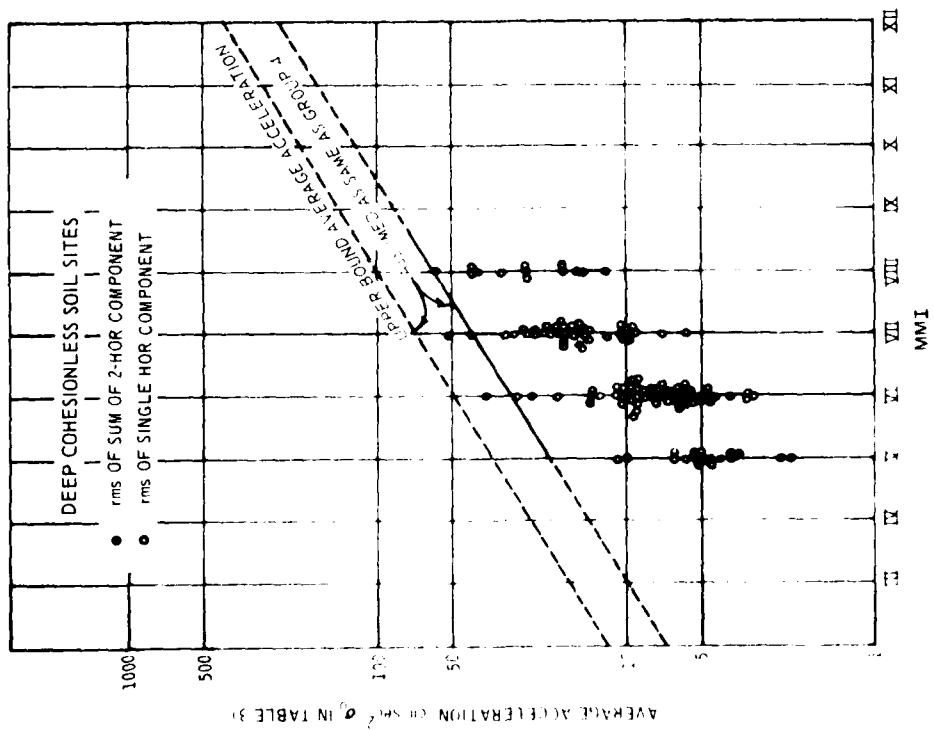
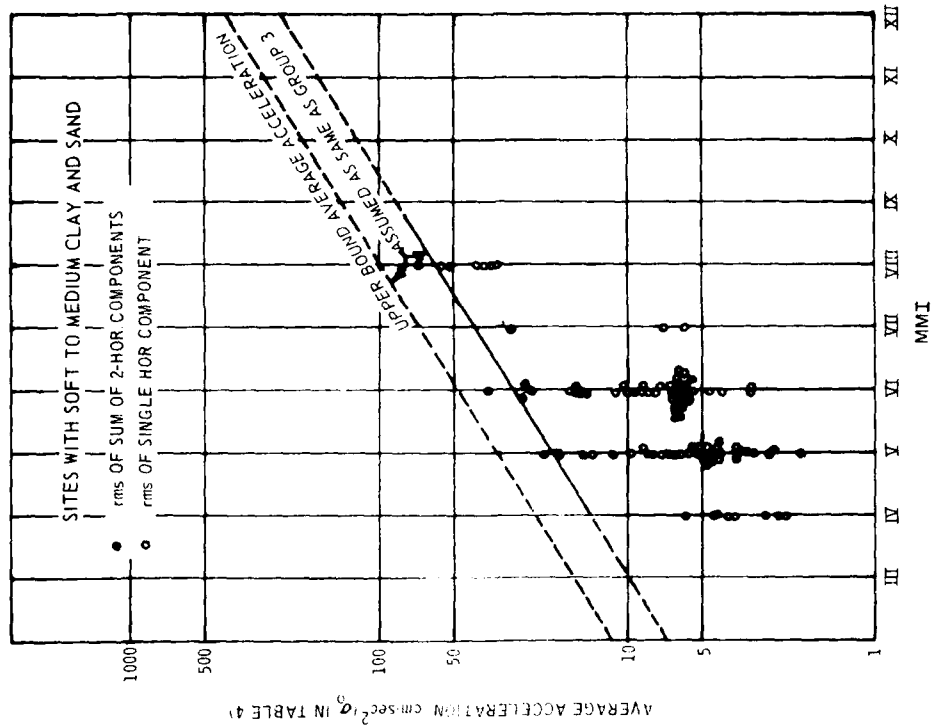


Figure 23. Correlation of upper-bound average acceleration versus MMI - soft sites (deep cohesionless soil and soft to medium clay and sand sites)

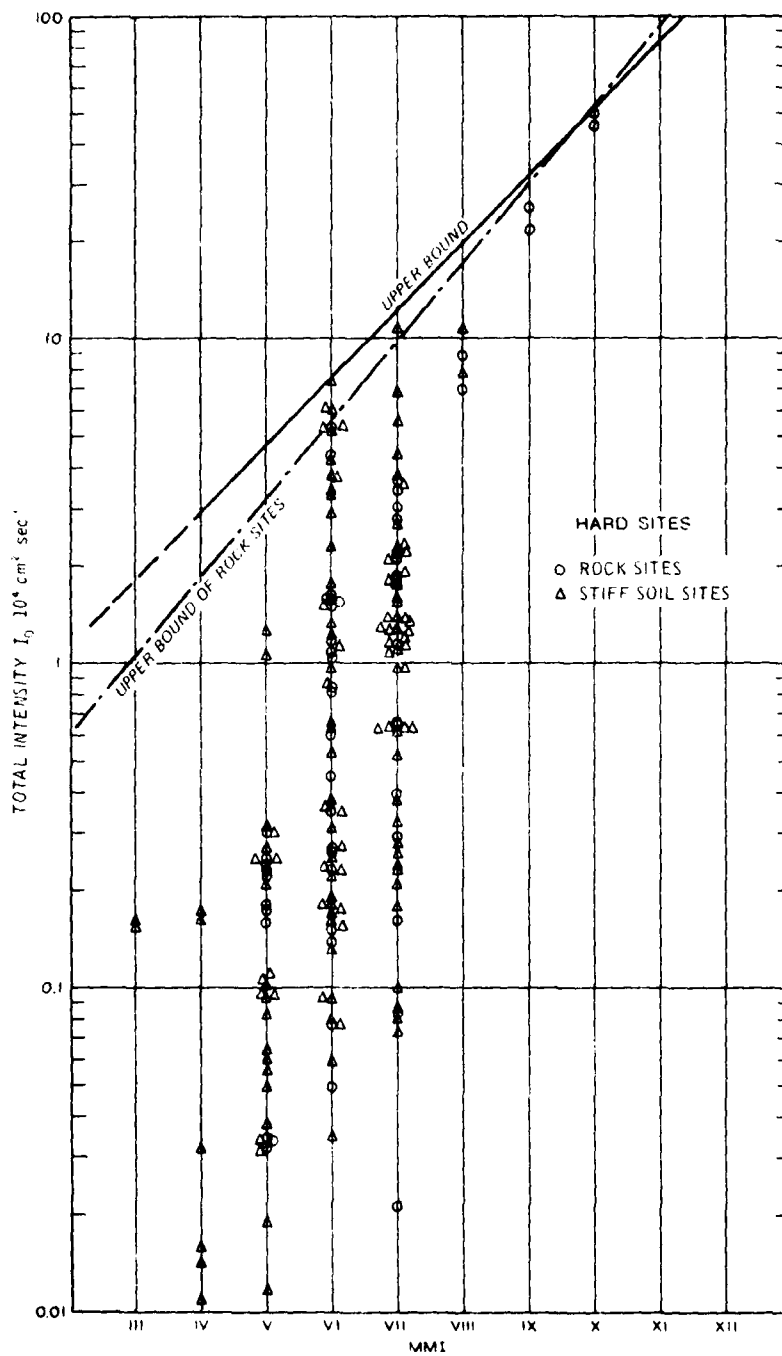


Figure 24. Probable seismic intensity  $I_0$  at epicentral region - hard sites

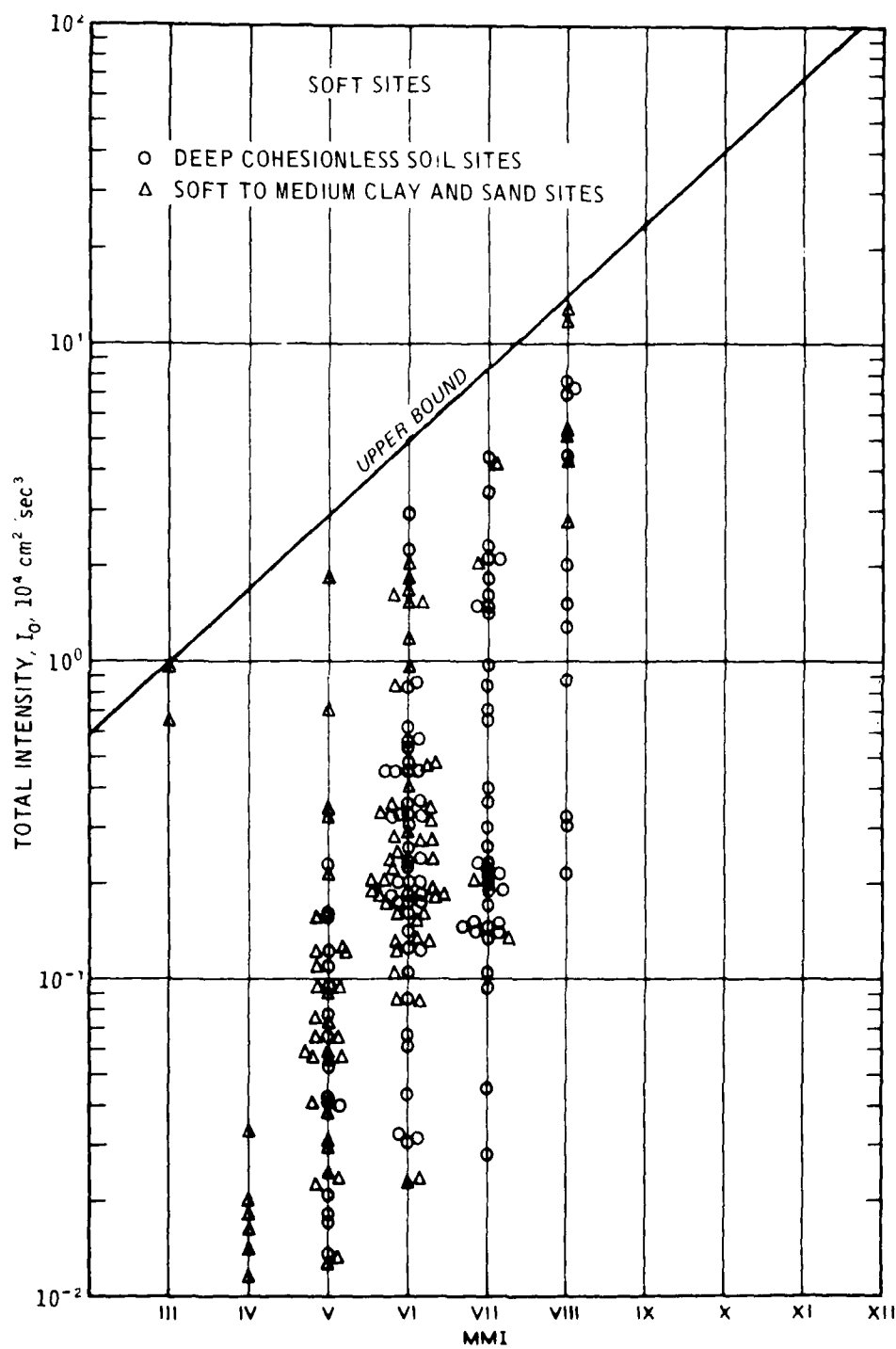


Figure 25. Probable seismic intensity  $I_0$  at epicentral region - soft sites

	Probable Seismic Epicentral Intensity	
	Hard Sites	Soft Sites
MMI	$10^4(\text{cm}^2/\text{sec}^3)$	$10^4(\text{cm}^2/\text{sec}^3)$
XII	135-160	120
XI	82-92	70
X	52-54	40
IX	30-34	24
VIII	17-20	14
VII	10-13	8
VI	6-8	5
V	3-5	3
IV	2-3	2

46. The upper-bound line of Figure 25 indicates that the seismic intensity at soft sites is lower than at hard sites. Also, the rate of attenuation is lower for soft sites than for hard sites. Of course, the upper-bound seismic intensities for the hard sites (Figure 24) and the soft sites (Figure 25) are in the near field. The data under the upper-bound line (both Figures 24 and 25) spread widely because of various earthquake magnitudes and distances.

47. Damage to structures in the epicentral area is generally more severe on soft sites than on hard sites, based on past experience and observations. However, this study showed the seismic total intensity (seismic energy) at soft sites to be lower than at hard sites. Thus, the degree of damage to structures does not correlate with the seismic total intensity in the epicentral region. Furthermore, the predominant frequencies at soft sites are in the range of 0 to 2.5 Hz; the seismic energy in this low-frequency range deserves further investigation as it relates to structural damage.

## PART VI: SUMMARY, CONCLUSIONS, AND RECOMMENDATIONS

### Summary

48. This study presents the results of a statistical analysis of the spectral shapes of PSD functions of 0 to 10 Hz for 421 ground accelerograms from 89 earthquakes, mostly in the western United States and Japan. The 421 horizontal accelerograms recorded on ground surface level have been divided into groups representing (a) rock sites (56 records), (b) stiff soil sites (131 records), (c) deep cohesionless soil sites (120 records), and (d) soft to medium clays and sands (114 records). The significant earthquake information (earthquake name, recording station, date, distance, magnitude, MMI, and peak acceleration), base average power  $\lambda^2$  (area under the PSD curve for the extended record of 163.82 sec), base average acceleration  $\lambda$ , conversion factor (ratio of 163.82 sec to the duration of the selected record, or strong-motion duration), raw average power  $\lambda_o^2$  (spectral intensity, area under the RPSD curve of the actual duration or the selected strong-motion duration), raw average acceleration  $\lambda_o$ , corrected average power  $\lambda_s^2$  (about 12.5 percent less than  $\lambda_o^2$ ), corrected average acceleration  $\lambda_s$ , and total intensity  $I_o$  for each record are listed in Tables 1-4. Values of  $\lambda_o^2$ , which were not directly estimated from original (actual) duration, were converted from  $\lambda^2$ . Generally,  $\lambda_o^2$  was about 12.5 percent higher than  $\lambda_s^2$ .

49. All 421 accelerograms were extended to 163.82 sec at an equal time interval  $\Delta t$  of 0.02 sec by adding a string of zero accelerations. Then, the statistical mean, standard deviation, etc., were calculated for the extended accelerogram and adjusted to a zero mean. Next, the PSD and the area under the PSD curve of the extended, zero-mean accelerogram (up to a frequency of 10 Hz) were estimated. Finally, the PSD curves were normalized to a unit area to contain NPSD curves. The statistical mean and mean plus one standard deviation of the NPSD curves for the four site conditions were established.

50. From the comparison of the four site-dependent NPSD spectra,



it is clear that there are differences in PSD spectral shapes depending on the site conditions. Two major groups are formed in the mean NPSD spectra: soft to medium clays and sands and deep cohesionless soil sites are similar and form one soft group; stiff soil and rock sites form one hard group. The frequency of 2.5 Hz (0.4-sec period) forms a dividing line on the frequency axis; in the frequency range lower than 2.5 Hz, spectral amplifications for the soft sites are much higher than the hard sites; and in the frequency range higher than 2.5 Hz, spectral amplifications for the hard sites are higher. However, in the case of mean plus one standard deviation NPSD spectra, the peak amplitudes in the low frequency range ( $<2.5$  Hz) decrease in the order of soft soil, deep cohesionless soil, stiff soil, and rock sites in accordance with the degree of hardness. This order seems in correlation with the damage.

51. In the soft group, the peak amplitude at about 1 Hz for the soft to medium clays and sands is about 14.3 percent higher than the deep cohesionless soils. Both of them are monotonically attenuated from the sharp peak at 1 to 10 Hz (except one hump at 2.75 Hz for the deep cohesionless soils). In the hard group, the largest peak amplitudes for the rock sites and stiff soil sites are at 2.75 Hz (0.36 sec) and 0.8 Hz (1.25 sec), respectively. Generally speaking, the energy content is spread widely over the frequency range of 0 to 10 Hz. It is possible that there is a connection between the largest peak amplitude at 2.75 Hz for the hard group and the hump at 2.75 Hz for the deep cohesionless soils or the soft group. In other words, it could be said that 2.75 Hz is a common frequency of bedrock under the deep cohesionless soils.

52. A qualitative comparison was made of the spectral shapes of PSD in this study with the Acceleration Response Spectra (ARS) of Seed and Idriss (1971), Seed, Ugas, and Lysmer (1976), and Kiremidjian and Shah (1978). There is general agreement in the spectral shapes of both methods except those for rock sites that the amplitude of the ARS of Seed, Ugas, and Lysmer (1976) was lower than for the PSD in the high frequency range. This discrepancy in amplitudes of spectra between the PSD and the ARS was due principally to the smaller number of records for the latter. The number of rock site records used was 28 for the ARS and

56 for the PSD. Thus, the average spectral amplitude value for the former is less reliable than the latter. Another difference is that the spectral shapes of the PSD function show more peaks than do the ARS.

53. The base average power  $\lambda^2$  (area) under the PSD curve, which is uniformly distributed on 163.82 sec of the extended record, has been established for each of the 421 records. The raw average power  $\lambda_o^2$ , or any average power of strong-motion duration (see Table 6), which is inversely proportional to the duration, can be easily calculated as  $\lambda^2$  times the ratio of 163.82 sec to the duration of the selected record.

54. The approximate linear relationships of the maximum ground accelerations  $a_{max}$  versus the base average accelerations  $\lambda$  and the average accelerations  $\lambda_o$  provide a set of scaling curves for the four site groups. Since the  $\lambda_o^2$  is the PSD spectral intensity, or the scaling factor, a PSD spectrum could be generated for any design earthquake based on this set of scaling curves and the four standard mean and mean plus one standard deviation NPSD spectra.

55. In the final analyses, close relationships do exist among the three parameters, duration, average acceleration, and peak ground acceleration. Duration is inversely proportional to the square of the average acceleration (average power). The latter has an approximate linear relation with the peak ground acceleration. It is apparent that duration has a large effect on the average acceleration or PSD spectral intensity  $\lambda_o^2$ , i.e., an engineering intensity scale. It is also the scaling factor for the normalized standard PSD spectrum. However, the average acceleration is a relative value that varies with duration; it is a scaling factor of the NPSD curve. It might be useful to take the Arias intensity  $I_o$  as a standard earthquake intensity scale. The Arias value includes the total duration and the average acceleration.

### Conclusions

56. The statistical analysis of 421 accelerograms shows clear differences in spectral shapes for different soil and geological conditions. Within the high-frequency range of 2.5 to 10 Hz, the spectrum

for the rock sites contains the highest energy or intensity; the spectrum of the stiff soil sites is slightly lower than for the rock sites; and the spectra of the soft clay and sand sites and the deep cohesionless soil sites are lower still and almost the same. However, in the low-frequency range of 0 to 2.5 Hz, the reverse exists: the soft sites indicate the highest energy, the deep cohesionless soil sites are next, the stiff soil sites are third, and finally, the rock sites. Generally, the spectra of rock sites and stiff soil sites of similar characteristics can be classified together as hard sites; the other two site types can be classified together as soft sites.

57. The site dependence of NPSD spectra have been established by statistical analysis as expected. The most significant finding of the study is the approximate linear correlation of the PGA ( $a_{\max}$ ) and average acceleration ( $\lambda_0$ ). Since  $\lambda_0^2$  is the area under the PSD curve, therefore  $\lambda_0^2$  can be used as a scaling factor for NPSD spectra. If  $a_{\max}$  is given,  $\lambda_0$  can be found from the correlation curves of  $a_{\max}$  and  $\lambda_0$ . The standard NPSD spectrum can be amplified by  $\lambda_0^2$  to become a design PSD spectrum.

58. The comparison of the attenuation curves of the PGA and the average acceleration versus distance of the San Fernando earthquake of 9 February 1971 showed that the attenuation rate of the average acceleration is less than the PGA and approximately linear on a log scale.

#### Recommendations

59. Further developments in the following three areas are needed:
- a. Generation of accelerograms based on the design PSD spectrum.
  - b. Relationships between the PSD spectrum and the response spectrum.
  - c. A new earthquake engineering intensity scale based on average acceleration or average power of strong-motion duration.

## REFERENCES

- Arnold, P. 1975. "The Influence of Site Azimuth and Local Soil Conditions on Earthquake Ground Motion Spectra," M.S. thesis, Massachusetts Institute of Technology, Cambridge, Mass.
- Arnold, P., and Vanmarcke, E. H. 1977. "Ground Motion Spectral Content: The Influence of Local Soil Conditions and Site Azimuth," Proceedings, Sixth World Conference on Earthquake Engineering, New Delhi, India, Vol 2, pp 113-118.
- Bendat, J. S., and Piersol, A. G. 1971. Random Data, Analysis and Measurement Procedures, Wiley-Interscience, New York.
- Blackman, R. B., and Tukey, J. W. 1958. The Measurement of Power Spectral, Dover Publications, Inc., New York.
- Bolt, B. A. 1978. "The Local Magnitude  $M_L$  of the Keon County Earthquake of July 21, 1952, Large Creep Events on Imperial Fault, California," Bulletin, Seismological Society of America, Vol 68, No. 2, pp 513-515.
- Berrill, J. B. 1977. "Site Effects During the San Fernando, California, Earthquake," Proceedings, Sixth World Conference on Earthquake Engineering, New Delhi, India, Vol 2, pp 101-106.
- California Institute of Technology. 1971-1975. "Strong-Motion Earthquake Accelerograms; Corrected Accelerograms and Integrated Ground Velocities and Displacements," Vol 2, Parts A-N, Earthquake Engineering Research Laboratory, Pasadena, Calif.
- Chang, F. K. 1978 (Apr). "State-of-the-Art for Assessing Earthquake Hazards in the United States; Catalogue of Strong-Motion Earthquake Records, Volume I, Western United States, 1933-1971," Miscellaneous Paper S-73-1, Report 9, U. S. Army Engineer Waterways Experiment Station, CE, Vicksburg, Miss.
- Chang, F. K., and Krinitzsky, E. L. 1977 (Dec). "State-of-the-Art for Assessing Earthquake Hazards in the United States; Duration, Spectral Content, and Predominant Period of Strong Motion Earthquake Records from Western United States," Miscellaneous Paper S-73-1, Report 8, U. S. Army Engineer Waterways Experiment Station, CE, Vicksburg, Miss.
- Duke, C. M., and Hradilek, P. J. 1977. "Spectral Analysis of Site Effects in the San Fernando Earthquake," Proceedings, Sixth World Conference on Earthquake Engineering, New Delhi, India, Vol 2, pp 680-690.
- Hsu, H. P. 1967. Outline of Fourier Analysis, Simon and Schuster, Inc., New York.
- Hudson, D. E. 1972. "Local Distributions of Strong Earthquake Ground Shaking," Bulletin, Seismological Society of America, Vol 62, No. 6, pp 1765-1786.
- Hudson, D. E., and Udawadia, F. E. 1974. "Local Distributions of Strong Earthquake Ground Motions," Proceedings, Fifth World Conference on Earthquake Engineering, Rome, Italy, Vol 1, pp 691-700.

Kiremidjian, A. S., and Shah, C. H. 1978. "Probabilistic Site-Dependent Response Spectra," Report No. 29, John A. Blume Earthquake Engineering Center, Department of Civil Engineering, Stanford, University, Stanford, Calif.

McCann, M. W., Jr., and Shah, C. H. 1979. "Determining Strong-Motion Duration of Earthquakes," Bulletin, Seismological Society of America, Vol 69, No. 4, pp 1253-1266.

Nuttli, O. W., Bollinger, G. A., and Griffiths, D. N. 1979. "On the Relation Between Modified Mercalli Intensity and Body-Wave Magnitude," Bulletin, Seismological Society of America, Vol 69, No. 3, pp 893-910.

Pereira, J., Oliverira, C. S., and Duarte, R. T. 1977. "Direct and Indirect Conversion from Power Spectra to Response Spectra," Proceedings, Sixth World Conference on Earthquake Engineering, New Delhi, India, Vol 2, pp 279-284.

Ravana, A. 1965. "Spectral Analysis of Seismic Actions," Proceedings, Third World Conference on Earthquake Engineering, New Zealand, Vol 1, pp 195-204.

Seed, H. B., and Idriss, I. M. 1971. "Influence of Soil Conditions on Building Damage Potential During Earthquakes," Journal, Structural Division, American Society of Civil Engineers, Vol 97, No. ST2, Proceedings Paper 7909, pp 639-663.

Seed, H. B., Ugas, C., and Lysmer, J. 1976. "Site-Dependent Spectra for Earthquake-Resistant Design," Bulletin, Seismological Society of America, Vol 66, pp 221-244.

Shannon and Wilson, Inc., and Agbabian Associates. 1976. "Site-Dependent Effects of Strong-Motion Accelerogram Stations," Progress Report prepared for U. S. Nuclear Regulatory Commission, Office of Nuclear Regulatory Research, Washington, D. C.

Tezcan, S. S. 1971. "Earthquake Design Formula Considering Local Soil Conditions," Journal, Structural Division, American Society of Civil Engineers, Vol 97, No. ST9, Proceedings Paper 8399, pp 2383-2405.

U. S. Nuclear Regulatory Commission, Office of Nuclear Reactor Regulation. "Design Response Spectral for Nuclear Power Plants," Regulatory Guide No. 1.60, Washington, D. C.

Vanmarcke, E. H. 1979 (Aug). "State-of-the-Art for Assessing Earthquake Hazards in the United States; Representation of Earthquake Ground Motion: Scaled Accelerograms and Equivalent Response Spectra," Miscellaneous Paper S-73-1, Report 14, U. S. Army Engineer Waterways Experiment Station, CE, Vicksburg, Miss.

Vanmarcke, E. H., and Cornell, C. A. 1972. "Seismic Risk and Design Response Spectra," American Society of Civil Engineers Specialty Conference on Safety and Reliability of Metal Structures, Pittsburgh, Pa.

Vanmarcke, E. H., and Gasparini, D. A. 1977. "Simulated Earthquake Ground Motions," Transactions, Fourth International Conference on Structural Mechanics in Reactor Technology, Vol K, pp 1-9.

Vanmarcke, E. H., and Lai, S. S. P. 1977. "Strong-Motion Duration of Earthquakes," Evaluation of Seismic Safety of Buildings, Publication No. R77-16, Report No. 10, Massachusetts Institute of Technology, Cambridge, Mass.

\_\_\_\_\_. 1980. "Strong-Motion Duration and R.M.S. Amplitude of Earthquake Records," Bulletin, Seismological Society of America, Vol 70, No. 4, pp 1293-1307.

Table 1  
Rock Sites[illegible]

(continued)

1949. Average cover = 1.60, 7.7, area under P<sub>1</sub> curve for the extended record of 16,947 sec.

corrective action, or corrective action, or corrective action.

1. The first step is to identify the problem or question that needs to be answered. This involves understanding the context and the specific requirements of the task.

1. The first step in the process is to identify the problem or issue that needs to be addressed. This involves gathering information and understanding the context of the problem.

[illegible]

Table 1 (Concluded)



1125

[illegible][illegible]

Table 2 (Continued)

[illegible]

© 1997 by Peter and Barbara C. Perreault, Inc. All rights reserved. These data.

Figure 1. The effect of the concentration of the *Agrobacterium* strain on the transformation efficiency of *Agrobacterium* strain 101. The concentration of the *Agrobacterium* strain 101 was varied from 10<sup>6</sup> to 10<sup>9</sup> cells/ml. The transformation efficiency was determined by the number of transformants per 10<sup>6</sup> cells of the *Agrobacterium* strain 101. The data are the mean  $\pm$  SD of three independent experiments. The asterisk indicates a significant difference from the control ( $P < 0.05$ ).

Record No.	Earthquake	Date	Mag.	Depth	Lat.	Long.	Modified Magnitude
1946	1946	11/11/69	6.2	10	33.4	156.0	6.2
1947	1947	03/11/69	6.2	10	33.4	156.0	6.2
1948	1948	03/11/69	6.2	10	33.4	156.0	6.2
1949	1949	03/11/69	6.2	10	33.4	156.0	6.2
1950	1950	03/11/69	6.2	10	33.4	156.0	6.2
1951	1951	03/11/69	6.2	10	33.4	156.0	6.2
1952	1952	03/11/69	6.2	10	33.4	156.0	6.2
1953	1953	03/11/69	6.2	10	33.4	156.0	6.2
1954	1954	03/11/69	6.2	10	33.4	156.0	6.2
1955	1955	03/11/69	6.2	10	33.4	156.0	6.2
1956	1956	03/11/69	6.2	10	33.4	156.0	6.2
1957	1957	03/11/69	6.2	10	33.4	156.0	6.2
1958	1958	03/11/69	6.2	10	33.4	156.0	6.2
1959	1959	03/11/69	6.2	10	33.4	156.0	6.2
1960	1960	03/11/69	6.2	10	33.4	156.0	6.2
1961	1961	03/11/69	6.2	10	33.4	156.0	6.2
1962	1962	03/11/69	6.2	10	33.4	156.0	6.2
1963	1963	03/11/69	6.2	10	33.4	156.0	6.2
1964	1964	03/11/69	6.2	10	33.4	156.0	6.2
1965	1965	03/11/69	6.2	10	33.4	156.0	6.2
1966	1966	03/11/69	6.2	10	33.4	156.0	6.2
1967	1967	03/11/69	6.2	10	33.4	156.0	6.2
1968	1968	03/11/69	6.2	10	33.4	156.0	6.2
1969	1969	03/11/69	6.2	10	33.4	156.0	6.2
1970	1970	03/11/69	6.2	10	33.4	156.0	6.2
1971	1971	03/11/69	6.2	10	33.4	156.0	6.2
1972	1972	03/11/69	6.2	10	33.4	156.0	6.2
1973	1973	03/11/69	6.2	10	33.4	156.0	6.2
1974	1974	03/11/69	6.2	10	33.4	156.0	6.2
1975	1975	03/11/69	6.2	10	33.4	156.0	6.2
1976	1976	03/11/69	6.2	10	33.4	156.0	6.2
1977	1977	03/11/69	6.2	10	33.4	156.0	6.2
1978	1978	03/11/69	6.2	10	33.4	156.0	6.2
1979	1979	03/11/69	6.2	10	33.4	156.0	6.2
1980	1980	03/11/69	6.2	10	33.4	156.0	6.2
1981	1981	03/11/69	6.2	10	33.4	156.0	6.2
1982	1982	03/11/69	6.2	10	33.4	156.0	6.2
1983	1983	03/11/69	6.2	10	33.4	156.0	6.2
1984	1984	03/11/69	6.2	10	33.4	156.0	6.2
1985	1985	03/11/69	6.2	10	33.4	156.0	6.2
1986	1986	03/11/69	6.2	10	33.4	156.0	6.2
1987	1987	03/11/69	6.2	10	33.4	156.0	6.2
1988	1988	03/11/69	6.2	10	33.4	156.0	6.2
1989	1989	03/11/69	6.2	10	33.4	156.0	6.2
1990	1990	03/11/69	6.2	10	33.4	156.0	6.2
1991	1991	03/11/69	6.2	10	33.4	156.0	6.2



[illegible][illegible]

period: 100.0

**PURI • Puri Vidyapeeth Research Institute**



7. *Journal of the American Medical Association*, 1975; 230: 1219-1220.

Record No.	Earthquake	Date	Mag.	Dist.	Max. Acc.	Max. Depth	Site	Estimated Damage	Notes
1	San Francisco	03/22/67	5.3	18	N45E	0.047	285	17.26	194,796
2	San Francisco	03/22/67	5.3	18	N45E	0.046	285	17.26	194,796
3	San Francisco	03/22/67	5.3	18	N45E	0.046	285	17.26	194,796
4	San Francisco	03/22/67	5.3	18	N45E	0.046	285	17.26	194,796
5	San Francisco	03/22/67	5.3	18	N45E	0.046	285	17.26	194,796
6	San Francisco	03/22/67	5.3	18	N45E	0.046	285	17.26	194,796
7	San Francisco	03/22/67	5.3	18	N45E	0.046	285	17.26	194,796
8	San Francisco	03/22/67	5.3	18	N45E	0.046	285	17.26	194,796
9	San Francisco	03/22/67	5.3	18	N45E	0.046	285	17.26	194,796
10	San Francisco	03/22/67	5.3	18	N45E	0.046	285	17.26	194,796
11	San Francisco	03/22/67	5.3	18	N45E	0.046	285	17.26	194,796
12	San Francisco	03/22/67	5.3	18	N45E	0.046	285	17.26	194,796
13	San Francisco	03/22/67	5.3	18	N45E	0.046	285	17.26	194,796
14	San Francisco	03/22/67	5.3	18	N45E	0.046	285	17.26	194,796
15	San Francisco	03/22/67	5.3	18	N45E	0.046	285	17.26	194,796
16	San Francisco	03/22/67	5.3	18	N45E	0.046	285	17.26	194,796
17	San Francisco	03/22/67	5.3	18	N45E	0.046	285	17.26	194,796
18	San Francisco	03/22/67	5.3	18	N45E	0.046	285	17.26	194,796
19	San Francisco	03/22/67	5.3	18	N45E	0.046	285	17.26	194,796
20	San Francisco	03/22/67	5.3	18	N45E	0.046	285	17.26	194,796
21	San Francisco	03/22/67	5.3	18	N45E	0.046	285	17.26	194,796
22	San Francisco	03/22/67	5.3	18	N45E	0.046	285	17.26	194,796
23	San Francisco	03/22/67	5.3	18	N45E	0.046	285	17.26	194,796
24	San Francisco	03/22/67	5.3	18	N45E	0.046	285	17.26	194,796
25	San Francisco	03/22/67	5.3	18	N45E	0.046	285	17.26	194,796
26	San Francisco	03/22/67	5.3	18	N45E	0.046	285	17.26	194,796
27	San Francisco	03/22/67	5.3	18	N45E	0.046	285	17.26	194,796
28	San Francisco	03/22/67	5.3	18	N45E	0.046	285	17.26	194,796
29	San Francisco	03/22/67	5.3	18	N45E	0.046	285	17.26	194,796
30	San Francisco	03/22/67	5.3	18	N45E	0.046	285	17.26	194,796
31	San Francisco	03/22/67	5.3	18	N45E	0.046	285	17.26	194,796
32	San Francisco	03/22/67	5.3	18	N45E	0.046	285	17.26	194,796
33	San Francisco	03/22/67	5.3	18	N45E	0.046	285	17.26	194,796
34	San Francisco	03/22/67	5.3	18	N45E	0.046	285	17.26	194,796
35	San Francisco	03/22/67	5.3	18	N45E	0.046	285	17.26	194,796
36	San Francisco	03/22/67	5.3	18	N45E	0.046	285	17.26	194,796
37	San Francisco	03/22/67	5.3	18	N45E	0.046	285	17.26	194,796
38	San Francisco	03/22/67	5.3	18</					

(continued)

1. The average power of the extended record of the 1960-1961 season is 1.65, which is 1.65 times the average power of the 1960-1961 season.

	4	5	6	7	8	9	10	11	12	13	14	15	16	17	18	19	20	21	22	23	24	25	26	27	28	29	30	31	32	33	34	35	36	37	38	39	40	41	42	43	44	45	46	47	48	49	50	51	52	53	54	55	56	57	58	59	60	61	62	63	64	65	66	67	68	69	70	71	72	73	74	75	76	77	78	79	80	81	82	83	84	85	86	87	88	89	90	91	92	93	94	95	96	97	98	99	100		
1	2	3	4	5	6	7	8	9	10	11	12	13	14	15	16	17	18	19	20	21	22	23	24	25	26	27	28	29	30	31	32	33	34	35	36	37	38	39	40	41	42	43	44	45	46	47	48	49	50	51	52	53	54	55	56	57	58	59	60	61	62	63	64	65	66	67	68	69	70	71	72	73	74	75	76	77	78	79	80	81	82	83	84	85	86	87	88	89	90	91	92	93	94	95	96	97	98	99	100

the device is similar to the one used in the previous study, but the rate of the saw is the electrically actuated duration of record length, converted to the rate of the saw.

1. The first step in the process of identifying a problem is to define the problem. This involves identifying the symptoms of the problem and determining the scope of the problem. Once the problem has been defined, the next step is to identify the causes of the problem. This involves identifying the factors that are contributing to the problem and determining the underlying causes. Once the causes have been identified, the next step is to develop a plan of action. This involves identifying the steps that need to be taken to solve the problem and determining the resources that will be needed to implement the plan. Once a plan of action has been developed, the next step is to implement the plan. This involves carrying out the steps that have been identified in the plan and monitoring the progress of the implementation. Finally, the last step in the process is to evaluate the results of the implementation. This involves determining whether the problem has been solved and whether the resources have been used effectively.

1000

1. The first group of respondents (n = 10) was composed of students who had completed the course and were currently employed in a related field. 2. The second group (n = 10) was composed of students who had completed the course and were currently employed in a non-related field. 3. The third group (n = 10) was composed of students who had completed the course and were currently unemployed. 4. The fourth group (n = 10) was composed of students who had completed the course and were currently employed in a related field. 5. The fifth group (n = 10) was composed of students who had completed the course and were currently employed in a non-related field. 6. The sixth group (n = 10) was composed of students who had completed the course and were currently unemployed. 7. The seventh group (n = 10) was composed of students who had completed the course and were currently employed in a related field. 8. The eighth group (n = 10) was composed of students who had completed the course and were currently employed in a non-related field. 9. The ninth group (n = 10) was composed of students who had completed the course and were currently unemployed. 10. The tenth group (n = 10) was composed of students who had completed the course and were currently employed in a related field.

[illegible][illegible]

1  
 2  
 3  
 4  
 5  
 6  
 7  
 8  
 9  
 10  
 11  
 12  
 13  
 14  
 15  
 16  
 17  
 18  
 19  
 20  
 21  
 22  
 23  
 24  
 25  
 26  
 27  
 28  
 29  
 30  
 31  
 32  
 33  
 34  
 35  
 36  
 37  
 38  
 39  
 40  
 41  
 42  
 43  
 44  
 45  
 46  
 47  
 48  
 49  
 50  
 51  
 52  
 53  
 54  
 55  
 56  
 57  
 58  
 59  
 60  
 61  
 62  
 63  
 64  
 65  
 66  
 67  
 68  
 69  
 70  
 71  
 72  
 73  
 74  
 75  
 76  
 77  
 78  
 79  
 80  
 81  
 82  
 83  
 84  
 85  
 86  
 87  
 88  
 89  
 90  
 91  
 92  
 93  
 94  
 95  
 96  
 97  
 98  
 99  
 100  
 101  
 102  
 103  
 104  
 105  
 106  
 107  
 108  
 109  
 110  
 111  
 112  
 113  
 114  
 115  
 116  
 117  
 118  
 119  
 120  
 121  
 122  
 123  
 124  
 125  
 126  
 127  
 128  
 129  
 130  
 131  
 132  
 133  
 134  
 135  
 136  
 137  
 138  
 139  
 140  
 141  
 142  
 143  
 144  
 145  
 146  
 147  
 148  
 149  
 150  
 151  
 152  
 153  
 154  
 155  
 156  
 157  
 158  
 159  
 160  
 161  
 162  
 163  
 164  
 165  
 166  
 167  
 168  
 169  
 170  
 171  
 172  
 173  
 174  
 175  
 176  
 177  
 178  
 179  
 180  
 181  
 182  
 183  
 184  
 185  
 186  
 187  
 188  
 189  
 190  
 191  
 192  
 193  
 194  
 195  
 196  
 197  
 198  
 199  
 200  
 201  
 202  
 203  
 204  
 205  
 206  
 207  
 208  
 209  
 210  
 211  
 212  
 213  
 214  
 215  
 216  
 217  
 218  
 219  
 220  
 221  
 222  
 223  
 224  
 225  
 226  
 227  
 228  
 229  
 230  
 231  
 232  
 233  
 234  
 235  
 236  
 237  
 238  
 239  
 240  
 241  
 242  
 243  
 244  
 245  
 246  
 247  
 248  
 249  
 250  
 251  
 252  
 253  
 254  
 255  
 256  
 257  
 258  
 259  
 260  
 261  
 262  
 263  
 264  
 265  
 266  
 267  
 268  
 269  
 270  
 271  
 272  
 273  
 274  
 275  
 276  
 277  
 278  
 279  
 280  
 281  
 282  
 283  
 284  
 285  
 286  
 287  
 288  
 289  
 290  
 291  
 292  
 293  
 294  
 295  
 296  
 297  
 298  
 299  
 300  
 301  
 302  
 303  
 304  
 305  
 306  
 307  
 308  
 309  
 310  
 311  
 312  
 313  
 314  
 315  
 316  
 317  
 318  
 319  
 320  
 321  
 322  
 323  
 324  
 325  
 326  
 327  
 328  
 329  
 330  
 331  
 332  
 333  
 334  
 335  
 336  
 337  
 338  
 339  
 340  
 341  
 342  
 343  
 344  
 345  
 346  
 347  
 348  
 349  
 350  
 351  
 352  
 353  
 354  
 355  
 356  
 357  
 358  
 359  
 360  
 361  
 362  
 363  
 364  
 365  
 366  
 367  
 368  
 369  
 370  
 371  
 372  
 373  
 374  
 375  
 376  
 377  
 378  
 379  
 380  
 381  
 382  
 383  
 384  
 385  
 386  
 387  
 388  
 389  
 390  
 391  
 392  
 393  
 394  
 395  
 396  
 397  
 398  
 399  
 400  
 401  
 402  
 403  
 404  
 405  
 406  
 407  
 408  
 409  
 410  
 411  
 412  
 413  
 414  
 415  
 416  
 417  
 418  
 419  
 420  
 421  
 422  
 423  
 424  
 425  
 426  
 427  
 428  
 429  
 430  
 431  
 432  
 433  
 434  
 435  
 436  
 437  
 438  
 439  
 440  
 441  
 442  
 443  
 444  
 445  
 446  
 447  
 448  
 449  
 450  
 451  
 452  
 453  
 454  
 455  
 456  
 457  
 458  
 459  
 460  
 461  
 462  
 463  
 464  
 465  
 466  
 467  
 468  
 469  
 470  
 471  
 472  
 473  
 474  
 475  
 476  
 477  
 478  
 479  
 480  
 481  
 482  
 483  
 484  
 485  
 486  
 487  
 488  
 489  
 490  
 491  
 492  
 493  
 494  
 495  
 496  
 497  
 498  
 499  
 500  
 501  
 502  
 503  
 504  
 505  
 506  
 507  
 508  
 509  
 510  
 511  
 512  
 513  
 514  
 515  
 516  
 517  
 518  
 519  
 520  
 521  
 522  
 523  
 524  
 525

\_\_\_\_\_

100







Table 5  
Comparison of Average Powers Estimated From Uncorrected, Corrected,  
and Extended 163.82-sec Duration Records

Row	Records and Duration	El Centro 1940		El Centro 1934		Taft 1952		Olympia 1949	
		N-S 30 sec	E-W 30 sec	N-S 25 sec	E-W 25 sec	N-S 30 sec	E-W 30 sec	N-S 30 sec	E-W 30 sec
		Average Power, $\text{cm}^2 \text{sec}^{-4}$							
(1)	Ravara* uncorrected	3820	2690	1900	2305	1360	1775	2930	2190
	Error (%) relative to (2)	19.6	17.6	57.3	65.9	39.0	65.9	38.5	59.3
(2)	CIT corrected (standard value)	3193	2288	1208	1389	978	1070	2116	1375
(3)	Extended 163.82 sec	3621	2637	1309	1502	1124	1219	2305	1525
	Error (%) relative to (2)	13.4	15.3	8.4	8.1	14.9	13.9	8.9	10.9
(4)	Final correction (3) $\times 0.875$	3168	2307	1145	1314	983	1067	2017	1334
	Accuracy of this study (%) relative to (2)	0.8	0.8	5.2	5.4	0.51	0.3	4.7	3.0

\* From Ravara (1965).

Example: Conversion Factor =  $\frac{\text{Extended record length (sec)}}{\text{Actual or selected length (sec)}}$

$$= \frac{163.82}{30.0}$$

$$= 5.46 \text{ for El Centro, 1940}$$

Average power for N-S component at duration 30 sec = Base\* average power for 163.82 sec duration (Column 10)  $\times$  conversion factor

$$= 663.2 \text{ (from Table 2)} \times 5.46$$

$$= 3621 \text{ cm}^2 \text{sec}^{-4} \text{ (in 3rd column of Row 3)}$$

Final corrected average power due to adding zeros =  $3621 \times 0.875$

$$= 3168 \text{ cm}^2 \text{sec}^{-4} \text{ (in 3rd column of Row 4)}$$

Table 6

Comparison of Variances Estimated in Same Duration by Vanmarcke and Lai and This Study

Record* No.	CIT No.	Earthquake	Instr. Comp.	Richter Magnitude	Max. Acc. g	Base Avg Power at Extended 163.82 sec cm <sup>2</sup> /sec <sup>4</sup>	Strong- Motion Duration S <sub>0</sub> ** sec	Converting Factor 163.82/S <sub>0</sub>	Variance ( $\sigma_o^2$ ) and rms Acc	
									This Study	Vanmarcke and Lai†
									$\frac{\sigma_o^2}{2}$ cm <sup>2</sup> /sec <sup>2</sup>	$\frac{\sigma_o^2}{2}$ cm <sup>2</sup> /sec <sup>2</sup>
3-31	A002-1	Northwest Calif. 10/7/51	S 44 W	6.0	0.104	33.818	3.78	43.3386	1,465.6	1,485.7
3-32	A002-2		N 46 W		0.112	42.639	4.19	39.0978	1,667.1	1,681.8
1-3	A004-1	Kern County 7/21/52 (Taft)	N 21 E	7.7	0.156	205.919	10.28	15.9358	3,281.5	3,309.3
1-4	A004-2		S 69 E		0.179	223.411	8.34	19.6427	4,388.4	4,422.9
1-9	B037-1	Parkfield 6/27/66	N 65 W	5.6	0.269	115.376	1.89	86.6770	10,000.5	10,084.1
1-10	B037-2	(Temblor)	S 25 W		0.347	170.910	1.65	99.2848	16,968.8	17,054.5
3-17	C048-1	San Fernando 2/9/71 (8244 Union Blvd)	NS	6.6	0.255	484.058	8.99	18.2224	8,820.7	8,876.9
3-18	C048-2		EW		0.134	255.708	16.99	9.6421	2,465.6	2,479.6
									49.6	49.8

\* This is the record number in this study; i.e., Tables 1-4.

\*\* The values of strong-motion duration were calculated from  $I_0 = S_0 \sigma_o^2$  by Vanmarcke and Lai (1977), where  $\sigma_o^2 = \int_0^\infty G(w) dw$ .† This was calculated from the values of  $I_0$  of Vanmarcke and Lai (1977).

Table 7

## Statistical Characteristics of Earthquake Ground Motion

Condition	Maximum Ground Acceleration, g			Frequencies of Selected Peaks, PSD Hz	Nor. Max. PSD		Average Acceleration, cm/sec <sup>2</sup>		
	Acceleration, g		Mean		Mean + σ	Mean	S.D.	Var.	
	Mean	S.D.							
Rock	0.196	0.234	0.054	1.06	0.146	0.369	30.84	38.35	1444.8
				2.75	0.184	0.412			
				3.80	0.160	0.353			
				5.17	0.133	0.321			
Stiff soil	0.050	0.369	0.137	0.80	0.192	0.547	17.5	12.8	162.4
				2.45	0.180	0.412			
				5.20	0.127	0.327			
Deep cohesion-less soil	0.063	0.272	0.074	1.00	0.350	0.827	11.2	8.3	68.5
				2.80	0.190	0.445			
Soft to medium clay and sand	0.054	0.046	0.002	1.05	0.405	1.315	9.3	8.4	70.5
				4.58	0.089	0.266			

Table 8

Correlation of rms Intensity Versus MMI

Upper bound of the site-dependent rms intensity, $\text{cm/sec}^2$ (square root of the sum of 2-horizontal variances)		
<u>MMI</u>	<u>Site Conditions</u>	
	<u>Hard Sites</u>	<u>Soft Sites</u>
XII	400-550	250-400
XI	285-395	170-280
X	205-275	120-200
IX	145-190	84-140
VIII	105-140	59-100
VII	75-99	41-70
VI	54-70	29-50
V	37-50	20-35

In accordance with letter from DAEN-RDC, DAEN-ASI dated 22 July 1977, Subject: Facsimile Catalog Cards for Laboratory Technical Publications, a facsimile catalog card in Library of Congress MARC format is reproduced below.

Chang, Frank K.

Site effects on power spectral densities and scaling factors : final report / by Frank K. Chang (Geotechnical Laboratory, U.S. Army Engineer Waterways Experiment Station). -- Vicksburg, Miss. : The Station ; Springfield, Va. : available from NTIS, [1981].

57, [15] p. : ill. ; 27 cm. -- (Miscellaneous paper / U.S. Army Engineer Waterways Experiment Station ; GL-81-2)

Cover title.

"July 1981."

"Prepared for Office, Chief of Engineers, U.S. Army, under Project 4A161102AT22, Work Unit 00296."

Bibliography: p. 55-57.

1. Earthquakes. 2. Power spectra. 3. Spectrum analysis. I. United States. Army. Corps of Engineers. Office of the Chief of Engineers. II. U.S. Army Engineer Waterways Experiment Station. Geotechnical Laboratory. III. Title IV. Series: Miscellaneous paper (U.S. Army Engineer Waterways Experiment Station) ; GL-81-2.  
TA7.W34m no.GL-81-2

END  
DATE  
FILMED  
9/8  
DTIC

AD-A102 899 ARMY ENGINEER WATERWAYS EXPERIMENT STATION VICKSBURG--ETC F/6 8/11  
SITE EFFECTS ON POWER SPECTRAL DENSITIES AND SCALING FACTORS.(U)  
JUL 81 F K CHANG  
UNCLASSIFIED WES/MP/GL-81-2 NL

2 2

AD-A102 899



END  
DATE  
FILMED  
11-82  
DTIC



**SUPPLEMENTARY**

**INFORMATION**



DEPARTMENT OF THE ARMY  
WATERWAYS EXPERIMENT STATION, CORPS OF ENGINEERS  
P. O. BOX 631  
VICKSBURG, MISSISSIPPI 39180

IN REPLY REFER TO: WESGH

30 November 1981

AD-A162899

Errata Sheet

No. 1

SITE EFFECTS ON POWER SPECTRAL DENSITIES

AND

SCALING FACTORS

Miscellaneous Paper GL-81-2

July 1981

1. Page 29, Figure 9: Change the horizontal scale of 0.1, 1, and 10 to 1, 10, and 100.
2. Page 31, Figure 11: Change the horizontal scale of 1, 10, and 100 to 0.1, 1, and 10.
3. Page 55, References: Line 16, change Keon County to Kern County.